

# Nonlinear Concept Erasure: a Density Matching Approach

Antoine Saillenfest<sup>a,\*</sup> and Pirmin Lemberger<sup>a,\*\*</sup>

<sup>a</sup>onepoint, 29 rue des Sablons, 75116 Paris (France)

**Abstract.** Ensuring that neural models used in real-world applications cannot infer sensitive information, such as demographic attributes like gender or race, from text representations is a critical challenge when fairness is a concern. We address this issue through concept erasure, a process that removes information related to a specific concept from distributed representations while preserving as much of the remaining semantic information as possible. Our approach involves learning an orthogonal projection in the embedding space, designed to make the class-conditional feature distributions of the discrete concept to erase indistinguishable after projection. By adjusting the rank of the projector, we control the extent of information removal, while its orthogonality ensures strict preservation of the local structure of the embeddings. Our method, termed  $\overline{\text{LEOPARD}}$ , achieves state-of-the-art performance in nonlinear erasure of a discrete attribute on classic natural language processing benchmarks. Furthermore, we demonstrate that  $\overline{\text{LEOPARD}}$  effectively mitigates bias in deep nonlinear classifiers, thereby promoting fairness.

## 1 Introduction

Pre-trained distributed representations, or embeddings, capture similarity or semantic meaning and are widely used in numerous machine learning applications. In certain critical scenarios, preventing a system from encoding specific concepts poses a significant challenge. A substantial body of research in fairness focuses on learning representations that exclude sensitive concepts, such as demographic attributes like gender or race [25, 5, 3]. Similarly, in explainability research, removing a concept from a model’s internal representation enables estimating its causal effect on a given task [13, 1, 18]. Consequently, there is growing interest in developing methods for learning representations that disentangle underlying concepts.

In this paper, we address the task of nonlinear concept erasure [24], which involves balancing two competing objectives: first removing concept-related information from a set of representations to ensure they are no longer predictive of the concept after erasure, and second, preserving as much information as possible from the original representation space. Nonlinear erasure refers to the impossibility for a nonlinear predictor, such as an MLP, to recover the concept after erasure. Our focus is on erasing discrete concepts, including demographic attributes such as gender or race. Specifically, we investigate post-hoc concept erasure, where representations are fixed and

\* Corresponding Author. Email: a.saillenfest@groupeonepoint.com.

\*\* Corresponding Author. Email: p.lemberger@groupeonepoint.com.

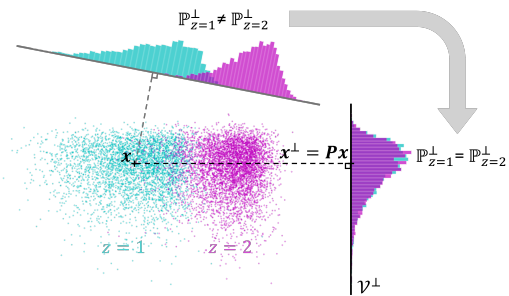


**Figure 1:**  $\overline{\text{LEOPARD}}$  erases a discrete attribute  $z$  by learning an orthogonal projection  $P$  onto a subspace  $\mathcal{V}^\perp$  of the feature space in which the distributions of the projected samples  $x^\perp = Px$  are indistinguishable across values of the protected attribute to erase  $z$ .

pre-trained (e.g., GloVe [22] or BERT embeddings [11] in NLP). Importantly, we tackle concept erasure in an unconstrained setting, which means that post-erasure representations are not optimized for any predefined downstream task.

We propose a simple yet novel concept erasure method which learns an orthogonal projection in the embedding space. The optimization process is driven by a density-matching erasure objective, ensuring that the class-conditional distributions of the representations after erasure are indistinguishable. The projection rank can be adjusted to control the extent of information removal. Leveraging orthogonal projections satisfies the dual objective of achieving non-invertible erasure while preserving the local structure of the feature space. We refer to our framework as  $\overline{\text{LEOPARD}}$ : **Non-Linear** concept Erasure via **Orthogonal Projection** and **Alignment** of post-erasure **Representation Distributions**. To evaluate the effectiveness of our approach, we conducted experiments demonstrating state-of-the-art performance in discrete concept erasure for the task of demographic attribute removal on standard NLP benchmarks. Furthermore, we show empirically that  $\overline{\text{LEOPARD}}$  can improve fairness of downstream classifiers with moderate impact on their performance. Our contributions are:

- We introduce  $\overline{\text{LEOPARD}}$ , a novel method for unconstrained nonlinear concept erasure relying on orthogonal projections and a class-conditional density matching objective.
- We demonstrate that  $\overline{\text{LEOPARD}}$  achieves state-of-the-art performance on many NLP benchmarks for the task of demographic attributes erasure.
- We demonstrate the utility of  $\overline{\text{LEOPARD}}$  in improving the fairness of deep classifiers with a moderate impact on performance.

## 2 Related work

Linear concept erasure is a restriction of concept erasure where adversaries are assumed to use linear predictors only to recover the concept after erasure. Some approaches use adversarial methods to learn projections that erase concepts [23, 24]. More recently, closed-form solutions for linear concept erasure have been proposed, eliminating altogether the need for learning an erasure function [24, 5]. These projections remove an optimal number of dimensions solely determined by the number of concept classes, which is usually small. High rank orthogonal projection naturally preserve the local structure of the embeddings. However, these methods struggle to fully remove concept-related information, as nonlinear predictors can still recover the concept after erasure [25]. Our method also involves learning projections but addresses the general problem of nonlinear concept erasure.

Nonlinear concept erasure remains largely an open problem. Recent efforts can be grouped into three main approaches. The first two are adversarial approaches relying on a gradient reversal layer during training [15, 13], and kernelized extensions of linear erasure methods [12, 25]. Both fall short of fully removing the protected information [25]. The last one covers recent methods that have drawn on rate-distortion theory to achieve nonlinear erasure by dispersing embeddings within the same concept class, effectively decorrelating them [3, 4]. These two works however raise fundamental issues. First, relying on nonlinear erasure functions may be detrimental to concept-unrelated information preservation. Second, these works address concept erasure, which is non-invertible, by learning invertible functions, which only become nearly non-invertible after optimization. In this paper, we focus on learning erasure projector which are linear and non-invertible by design.

Constrained de-biasing, or erasure, refers to optimizing post-erasure representations for a predefined downstream task, such as a classification [3], or a more generic one, such as Masked Language Modeling (MLM) for language models fine-tuning [11, 13]. In contrast, downstream tasks are assumed unknown a priori in an unconstrained mode, making it essential to preserve semantic information for broad applicability. Semantic preservation is typically evaluated via semantic similarity tests (e.g., WordSim-353 [2], WHEAT [9]) or the preservation of the neighborhood structure [4]. This paper is a contribution to unconstrained erasure.

Another relevant line of research focuses on developing predictors for downstream tasks that are robust to interventions on protected variables. To ensure such invariance, Veitch et al. (2021), followed by subsequent works [20], propose a regularization procedure which depends on an underlying causal model. This model assumes the existence of a part of the input representation that is independent of the protected attribute. By penalizing discrepancies between relevant conditional output distributions, they enforce specific independence properties between the target variable and the predictive features. By contrast, our method modifies the input representations. We operate under the assumption that the target variable is not available a priori, and our objective is to extract a part of the embeddings that is independent of the protected concept.

Concept erasure is relevant to numerous applications, including bias mitigation for fairness [5, 13], causal analysis for explainability [1, 18], and semantic analysis [24]. End-to-end training is often limited by computational constraints or inaccessible internal model parameters. As a result fixed, pre-trained representations remain widely used for their versatility across domains. Most existing approaches are evaluated on text embeddings from pre-trained models

like GLOVE [22], BERT [11], or GPT [8] or on image representations [24, 4]. The simplest setting for erasure involves categorical concepts, which encompass a wide range of applications, such as the removal of demographic biases related to gender or race in text embeddings [7, 10, 3, 4]. This paper focuses on *post-hoc* discrete concept erasure, assuming fixed and pre-trained embeddings.

## 3 Learning Projections with a Density Matching Objective

This section presents our optimization method,  $\bar{\text{LEOPARD}}$ , which aims to achieve nonlinear erasure of a discrete concept from a set of representations through orthogonal projections. We first introduce a parametrization for learning an orthogonal projection of prescribed rank, and subsequently introduce a density matching criterion to select the projection that best removes the concept information.

Let  $\mathcal{D} = \{x_i\}_{i=1}^N$  denote a dataset of representations in  $\mathbb{R}^d$  sampled i.i.d. from an underlying distribution  $\mathbb{P}$ . Each representation  $x_i$  is associated with a discrete class label  $z_i \in \mathcal{Z} := \{1, \dots, K\}$  corresponding to the concept to be erased. Let  $\mathcal{C} = \{z_i\}_{i=1}^N$ . We define the class-specific subset  $\mathcal{D}_{z=j} = \{x_i \in \mathcal{D} | z_i = j\}$ , so that  $\mathcal{D} = \bigcup_{j=1}^K \mathcal{D}_{z=j}$ , and let  $n_{z=j} = |\mathcal{D}_{z=j}|$  denote the cardinality of each subset. We denote by  $\mathbb{P}_{z=j} := \mathbb{P}(\cdot | z = j)$  the class-conditional distribution of samples.

### 3.1 Learning Orthogonal Projections

Our approach follows the linear bias subspace hypothesis, which posits that, for a given set of representations, the information related to a specific concept is entirely contained within a subspace of the embedding space [7, 27]. Consequently, we seek an orthogonal decomposition of the embedding space  $\mathbb{R}^d$  as  $\mathbb{R}^d = \mathcal{V}^\perp \oplus \mathcal{V}^\parallel$  where  $\mathcal{V}^\perp$  is the subspace of dimension  $r$  that is to be preserved, and  $\mathcal{V}^\parallel$  is its orthogonal complement of dimension  $d - r$  that is to be neutralized.

Since concept erasure is inherently a non-invertible operation, we enforce the erasure map to be non-invertible as well. Additionally, for simplicity we constrain the erasure map to be linear. Specifically, to ensure that the semantic content of the embeddings is maintained after erasure, we aim to preserve the local geometry of the embeddings through erasure, i.e., the distances between embeddings. This constrains the erasure function to be an orthogonal projection onto  $\mathcal{V}^\perp$ . Such a projection is fully characterized by a symmetric, idempotent matrix  $P \in \mathbb{R}^{d \times d}$  of rank  $r$  satisfying  $P^\top = P$  and  $P^2 = P$ . Let  $x^\perp$  denote the post-erasure representation of a representation  $x$ . The erasure operation is given by:

$$x^\perp = Px. \quad (1)$$

Standard linear algebra states that any rank- $r$  orthogonal projection matrix  $P$  admits the decomposition:

$$P = UU^\top, \quad (2)$$

where  $U \in \mathbb{R}^{d \times r}$  is a matrix with orthonormal columns, i.e.  $U^\top U = I_r$ , where  $I_r$  is the  $r \times r$  identity matrix.

In the context of an optimization process, the parametrization from Eq. 2 allows us to learn  $U$ , and consequently  $P$ , under the orthonormality constraint. To encourage this constraint during training, we define a *projection loss* to be minimized as:

$$\mathcal{L}_p(U) = \|U^\top U - I_r\|_F^2, \quad (3)$$

where  $\|\cdot\|_F$  denotes the Frobenius norm.

### 3.2 Class-Conditional Density Matching

To ensure that the learned projection effectively removes concept-specific information, we propose a criterion based on matching class-conditional distributions of the erased representations. Specifically, we aim for the post-erasure class-conditional distributions  $\mathbb{P}_{z=j}^\perp := \mathbb{P}_{z=j}(\cdot^\perp)$  to be indistinguishable across protected attribute classes.

We first consider the binary case  $\mathcal{Z} = \{1, 2\}$ . Let  $\mathbb{P}_{z=1}^\perp$  and  $\mathbb{P}_{z=2}^\perp$  denote the post-erasure distributions corresponding to  $z = 1$  and  $z = 2$ , respectively. Our objective is to minimize a divergence measure  $\text{dist}(\mathbb{P}_{z=1}^\perp, \mathbb{P}_{z=2}^\perp)$  between these two distributions. To quantify this distance, we use the Maximum Mean Discrepancy (MMD), chosen for its practical estimation from finite samples [16]. MMD simply computes the distance between the means of the embeddings of the distributions in a reproducing kernel Hilbert space (RKHS)  $\mathcal{H}$  associated with a positive-definite kernel  $k : \mathbb{R}^d \times \mathbb{R}^d \rightarrow \mathbb{R}$ . The unbiased empirical estimator of  $\text{MMD}^2$  [16] is given by:

$$\begin{aligned} \widehat{\text{MMD}}^2(\mathbb{P}_{z=1}^\perp, \mathbb{P}_{z=2}^\perp) &= \frac{1}{n_{z=1}(n_{z=1}-1)} \sum_{\substack{x, x' \in \mathcal{D}_{z=1} \\ x \neq x'}} k(x^\perp, x'^\perp) \\ &+ \frac{1}{n_{z=2}(n_{z=2}-1)} \sum_{\substack{x, x' \in \mathcal{D}_{z=2} \\ x \neq x'}} k(x^\perp, x'^\perp) \\ &- \frac{2}{n_{z=1}n_{z=2}} \sum_{x \in \mathcal{D}_{z=1}} \sum_{x' \in \mathcal{D}_{z=2}} k(x^\perp, x'^\perp). \end{aligned} \quad (4)$$

A common choice of kernel is the Gaussian kernel, defined as  $k(x, y) = \exp(-\frac{1}{2\sigma^2} \|x - y\|^2)$ , where  $\sigma > 0$  is a bandwidth parameter. This kernel has a feature expansion that includes an infinite number of terms, thereby capturing all orders of statistics. In this case the MMD distance between the two distributions vanishes if and only if they coincide.

In the context of an optimization procedure, the empirical estimator introduced above naturally induces an objective function, we refer to as the *erasure loss*, which is to be minimized with respect to the parameters  $U$  defining the erasure function:

$$\mathcal{L}_{\text{MMD}}(U; \mathcal{D}, \mathcal{C}) := \widehat{\text{MMD}}^2(\mathbb{P}_{z=1}^\perp, \mathbb{P}_{z=2}^\perp). \quad (5)$$

In the general case of a concept that can take more than two values, i.e.  $K \geq 2$ , a natural generalization of the density matching objective in Eq. 5 is to consider the sum of pairwise discrepancies:

$$\mathcal{L}_{\text{MMD}}(U; \mathcal{D}, \mathcal{C}) := \sum_{\substack{i, j \in \mathcal{Z} \\ i < j}} \widehat{\text{MMD}}^2(\mathbb{P}_{z=i}^\perp, \mathbb{P}_{z=j}^\perp). \quad (6)$$

As a side note, let us observe that, as stated in Belrose et al. (2023), one condition for linearly erasing a concept is that  $\mathbb{E}_{x \sim \mathbb{P}}[x^\perp | z = j] = \mathbb{E}_{x \sim \mathbb{P}}[x^\perp]$  for all concept classes  $j$ . In the context of steering, a problem closely related to erasure, Singh et al. (2024) extend prior conditioning approaches to enforce the equality of mean and variance of class-conditional distributions, deriving a closed-form solution that corresponds to minimizing the Wasserstein distance under Gaussian assumptions. Our density matching objective can be viewed as a much stronger constraint on the class-conditional distributions which pushes them towards being indistinguishable.

---

#### Algorithm 1 $\overline{\text{LEOPARD}}$

---

- 1: **Input:** Dataset  $\mathcal{D} = \{x_i\}_{i=1}^N$ , concept labels  $\mathcal{C} = \{z_i\}_{i=1}^N$ , rank  $r$ , mixing coefficient  $\gamma \in \mathbb{R}^+$ , initial matrix  $U^{(0)} \in \mathbb{R}^{d \times r}$ , number of training epochs  $N_e$
  - 2: **Output:** Rank- $r$  orthogonal projection matrix  $P$
  - 3: **for**  $i = 1$  **to**  $N_e$  **do**
  - 4:   Compute gradient:  $\nabla_U (\gamma \mathcal{L}_p(U) + \mathcal{L}_{\text{MMD}}(U; \mathcal{D}, \mathcal{C}))$
  - 5:   Update  $U$  via gradient descent
  - 6: **end for**
  - 7: % Project onto the closest orthogonal projector to  $UU^\top$  in Frobenius norm
  - 8:  $U, \Lambda = \text{EigenDecomposition}(UU^\top)$
  - 9:  $U_r \leftarrow U[:, 1:r]$
  - 10:  $P \leftarrow U_r U_r^\top$
- 

---

#### Algorithm 2 Cascaded $\overline{\text{LEOPARD}}$

---

- 1: **Input:** Dataset  $\mathcal{D} = \{x_i\}_{i=1}^N$ , concept labels  $\mathcal{C} = \{z_i\}_{i=1}^N$ , rank  $r$ , mixing coefficient  $\gamma \in \mathbb{R}^+$ , initial matrix  $U^{(0)} \in \mathbb{R}^{(d-K+1) \times r}$ , number of training epochs  $N_e$
  - 2: **Output:** Rank- $r$  orthogonal projection matrix  $P$
  - 3: Compute the orthogonalized LEACE projection  $P_L$
  - 4: Compute  $U_L \in \mathbb{R}^{d \times (d-K+1)}$  such that  $P_L = U_L U_L^\top$  and  $U_L^\top U_L = I_{d-K+1}$
  - 5: Erase the concept via  $\overline{\text{LEOPARD}}$  using Algorithm 1:  
 $P' = \overline{\text{LEOPARD}}(\{U_L^\top x_i\}_{i=1}^N, \mathcal{C}, r, \gamma, U^{(0)}, N_e)$
  - 6: Compose the final orthogonal projection:  $P \leftarrow U_L P' U_L^\top$
  - 7: %  $P$  is a rank- $r$  orthogonal projection:  $P = P^\top$ ,  $P^2 = P$   
and  $\text{rank}(P) = \text{rank}(P') = r$
- 

### 3.3 $\overline{\text{LEOPARD}}$

The optimization procedure for  $\overline{\text{LEOPARD}}$  is outlined in Algorithm 1. The goal is to learn a rank- $r$  orthogonal projection  $P$  that erases a discrete concept nonlinearly, parameterized via a matrix  $U \in \mathbb{R}^{d \times r}$  such that  $P = UU^\top$ , as in Eq. 2. The learning objective to minimize during training combines the *projection loss*  $\mathcal{L}_p$  (Eq. 3) and the *erasure loss*  $\mathcal{L}_{\text{MMD}}$  (Eq. 6) and is given by:

$$\mathcal{L}(U; \mathcal{D}, \mathcal{C}) = \gamma \mathcal{L}_p(U) + \mathcal{L}_{\text{MMD}}(U; \mathcal{D}, \mathcal{C}), \quad (7)$$

where the mixing coefficient  $\gamma > 0$  balances the two objectives.

At convergence, the matrix  $P = UU^\top$  is not guaranteed to be exactly idempotent due to approximate enforcement of orthogonality constraints. To ensure that the final output is a valid rank- $r$  orthogonal projector, we compute the closest orthogonal projection matrix in Frobenius norm to the approximate projection matrix  $UU^\top$  at the end of the training loop. This is achieved by performing an eigen-decomposition of  $UU^\top$  and retaining the top  $r$  eigenvectors to construct a semi-orthogonal matrix  $U_r$ , yielding the final orthogonal projection matrix  $P \leftarrow U_r U_r^\top$ .

The orthogonal projector  $P$  obtained through this procedure preserves the local geometric structure (i.e. the pairwise distances), a desirable property in representation spaces. In contrast, the approximate projection  $UU^\top$  at the end of training, while potentially achieving better concept erasure, lacks guaranteed idempotence. The extent to which the final orthogonal projection retains the erasure properties of the approximate solution depends on their proximity in Frobenius norm which is quantified precisely by the final value of the projection loss  $\mathcal{L}_p(U)$  (see Supplementary Material B for a proof).

The number of trainable parameters in  $\overline{\text{LEOPARD}}$  is  $d \cdot r$ , significantly lower than that of existing nonlinear erasure methods such as FaRM [3] and KRaM [4], which involve training multi-layer perceptrons for concept removal.

In  $\overline{\text{LEOPARD}}$ , the adjustable rank  $r$  governs the trade-off between the preservation of information and the effectiveness of concept removal. There does not exist a universally optimal value for  $r$ ; the rank adjustability constitutes a key strength of our method, enabling trade-offs between erasure and information preservation that are not possible with more rigid approaches.

**Cascaded  $\overline{\text{LEOPARD}}$**  The erasure objective introduced in Section 3.2 minimizes the MMD distance between class-conditional distributions. With a characteristic kernel (as in 3.2), this encourages alignment of all moments. However, MMD-based matching does not explicitly enforce mean alignment, which is essential for effective linear erasure [5]. As a result, the learned projection may fail to fully remove the targeted concept in a linear sense. To address this, we incorporate recent advances in concept erasure that ensure linear removal by construction, with negligible computational overhead.

*Cascaded erasure* is a two-stage process that integrates linear and nonlinear erasure. In the first stage, we apply an orthogonalized LEACE projection [5] to linearly remove the concept. The embeddings are then projected onto the  $(d - K + 1)$ -dimensional image subspace of this projection. In the second stage, these linearly "sanitized" embeddings are further processed using a nonlinear erasure method. When instantiated with  $\overline{\text{LEOPARD}}$ , it amounts to computing two orthogonal projections acting on nested subspaces. The overall cascaded projection remains orthogonal and inherits the benefits of both linear and nonlinear concept erasure. The full procedure for Cascaded  $\overline{\text{LEOPARD}}$  is outlined in Algorithm 2.

## 4 Experimental Setup

To evaluate our erasure method, we focus on the task of discrete concept erasure in text embeddings and its application to training fair classifiers. We compare our approach with SOTA methods for unconstrained nonlinear concept erasure FaRM [3] and KRaM [4].

Code and data : <https://github.com/toinesayan/non-LEOPARD>.

### 4.1 Datasets

**GLOVE** is a dataset derived from the GLOVE embeddings of the 150k most frequent words [22]. It includes a selection of words categorized as male-biased, female-biased, and neutral based on the magnitude of their projection onto the gender direction, the principal component of the vector space formed by gendered word-pair differences, treating gender as ternary. This dataset, used in [4], consists of 21,996 word embeddings stratified by gender, split 49%/21%/30% across training, validation, and test.

**BIAS IN BIOS** is a real world dataset suited for studying gender biases in biography classification tasks [10]. It consists in biographies collected through web scraping and labeled with binary gender and occupation (28 in total). We use the version from [23], which contains  $\sim 98\%$  of the original dataset, as the full version is no longer publicly available. It consists of 399,423 biographies stratified by occupation, split 65%/10%/25% across training, validation, and test.

**DIAL** is a Twitter-based sentiment classification dataset constructed from the DeepMoji corpus [6]. Each tweet is annotated with a binary sentiment label (*happy* or *sad*) and a "race" label, which corresponds to the linguistic style of the tweet (*African-American*

*English* (AAE) or *Standard American English* (SAE)). We use the version of the dataset made available by [4], which is balanced with respect to both race and sentiment labels. DIAL consists of 176k samples, split 91%/4.5%/4.5% across training, validation, and test.

### 4.2 Practical Aspects of MMD Evaluation

An important issue when using the MMD estimator with a Gaussian kernel in practice is the selection of the kernel bandwidth. To mitigate the necessity of tuning  $\sigma$  for each experiment, it is usual to rely on a heuristic [16]. In this study, we rely on the mean heuristic which consists in setting  $\sigma$  to be the pairwise mean distance on the aggregate sample, i.e.  $\sigma^2 = \frac{\sum_{x, x'} \|x - x'\|^2}{N^2 - N}$ .

Moreover, instead of a single kernel, we use a mixture of  $M$  kernels as in Li et al. (2015) to make MMD more adaptive and robust to distributional differences:

$$k(x, x') = \sum_{i=1}^M k_{\sigma_i}(x, x'), \quad (8)$$

where  $k_{\sigma_i}$  represents a Gaussian kernel with bandwidth  $\sigma_i$ . We set  $M = 5$  and  $\sigma_i = \alpha_i \sigma$ , with  $\alpha_i \in [\frac{1}{8}, \frac{1}{4}, \frac{1}{2}, 1.0, 2.0]$ .

The computational complexity of calculating the unbiased MMD<sup>2</sup> estimator with a mixture of  $M$  Gaussian kernels over a batch of  $b$  observations in  $\mathbb{R}^d$  is  $\mathcal{O}(b^2(d+M))$  when the bandwidth  $\sigma$  is estimated using the mean heuristic. The computation of all pairwise squared Euclidean distances dominates the bandwidth calculation step with a cost of  $\mathcal{O}(b^2d)$ . The subsequent evaluation of  $M$  kernels per pair adds  $\mathcal{O}(b^2M)$ . In terms of memory costs, storing  $b$  input data in  $\mathbb{R}^d$  and  $b^2$  pairwise distances yields a complexity of  $\mathcal{O}(bd + b^2)$ .

Large batch sizes may thus incur significant memory and computational costs during training but improve the accuracy of MMD<sup>2</sup> estimates. Based on available resources, we used large batches ( $b \geq 8192$ ) for GLOVE and BIAS IN BIOS, and a moderate size ( $b = 2048$ ) for DIAL. Smaller batches remain feasible, albeit with a slight reduction in performance. The above MMD design choices will be further discussed in Section 5.4.

### 4.3 Evaluation metrics

**Erasure evaluation.** Following prior works [12, 24, 4], we evaluate the quality of concept erasure by probing the learned representations for the target concept using nonlinear classifiers. A decrease in probing accuracy is an indicator of erasure. The closer you get to the accuracy of a random predictor, the better the erasure is presumed to be. We also report the Minimum Description Length (MDL) for predicting the erased concept after erasure which has been shown to be a reliable evaluation metric for erasure [29, 3]. MDL quantifies the *effort* required by a probing model to achieve a given performance. Higher MDL values suggest more effective erasure.

**Quantifying Post-Erasure Utility of the Representations.** When there is no predefined downstream task for which we can evaluate the accuracy, to measure the overall preservation of the semantic information in the embedding space we rely on the metric  $A_k$  introduced in [4] that quantifies the average overlap between the  $k$ -nearest neighbor sets of  $x_i$  and  $x_i^\perp$ . Formally,

$$A_k = \frac{1}{N} \sum_{x \in \mathcal{D}} \left[ \frac{1}{k} |k_{\text{nn}}(x) \cap k_{\text{nn}}(x^\perp)| \right], \quad (9)$$

where  $knn(\cdot)$  computes the  $k$ -nearest neighbor set of a representation. The metric ranges from 0 to 1, with values closer to 1 indicating greater preservation of the local geometry of the embeddings. We set  $k = \lfloor \frac{|D|}{2} \rfloor$ , denoting the average neighborhood overlap as  $A_{50\%}$ .

For datasets of words, like GLOVE, WordSim-353 (WS-353) Similarity Evaluation is a standard benchmark for assessing semantic representations by comparing model-predicted word similarities to human-annotated scores on 353 word pairs [2]. Model evaluation involves computing cosine similarity between word embeddings and correlating these scores with human ratings using Spearman’s rank correlation. For our analysis, we evaluated a subset of 196 word pairs where both words belong to the GLOVE vocabulary of the 150k most frequent words and have human similarity ratings available.

**Downstream Fairness Evaluation.** A direct application of concept erasure is the improvement of fairness in downstream classifiers by training them on post-erasure representations. To measure downstream classifier bias in BIAS IN BIOS and DIAL, we follow DeArteaga et al. (2019) and report the TPR-Gap metric, which quantifies bias by computing the difference (Gap) in the true positive rate (TPR) between individuals with different groups. Formally, let  $Z, Y$ , and  $\hat{Y}$  be random variables denoting respectively a binary protected attribute taking values in  $\{c, c'\}$ , the downstream task label taking values in  $\mathcal{Y}$ , and a model’s prediction on this task. Then the TPR-Gap  $GAP_{c;y}^{TPR}$  for a downstream task label  $y$  and a protected concept label  $c$  is:

$$\begin{aligned} TPR_{c,y} &= p(\hat{Y} = y | Z = c, Y = y) \\ GAP_{c;y}^{TPR} &= TPR_{c,y} - TPR_{c',y} \end{aligned} \quad (10)$$

In BIAS IN BIOS (resp. DIAL), the concept to erase is the binary gender (resp. race) and  $y$  is a profession (resp. a sentiment). Additionally, we consider  $GAP_c^{TPR,RMS}$  as the root mean square (RMS) of the TPR-Gap across all labels in  $\mathcal{Y}$  for a given concept class  $c$ . To explore the relationship between the bias exhibited by the model and the bias in the data, we also compute for BIAS IN BIOS  $\sigma_{GAP^{TPR},\%c}$ , the correlation between the TPR-Gap for a given profession and the percentage of individual with gender  $c$  in that profession.

TPR-GAP may be bad for evaluating fairness in real-world scenarios when  $Y$  and  $Z$  are highly correlated, as strong debiasing would inevitably lead to a degradation in downstream task performance. For completeness, we also report demographic parity which measures the difference in prediction w.r.t. to a protected attribute:

$$DP = \sum_{y \in \mathcal{Y}} |p(\hat{Y} = y | Z = c) - p(\hat{Y} = y | Z = c')| \quad (11)$$

#### 4.4 Implementation Details

Key implementation details are summarized below; additional information is provided in Supplementary Material C. All models are trained on an NVIDIA GeForce RTX 2080 Ti GPU with 11GB of VRAM using CUDA for accelerated computation.

We reimplemented FaRM [3] and KRaM [4]. Concept erasure is performed using a 4-layer MLP with ReLU activations for GLOVE and BIAS IN BIOS, and a 7-layer MLP for DIAL. For LEACE, we relied on a publicly available implementation.<sup>1</sup>

For BIAS IN BIOS, each input is represented by the final hidden state of a frozen BERT model (bert-base-uncased) [11] extracted

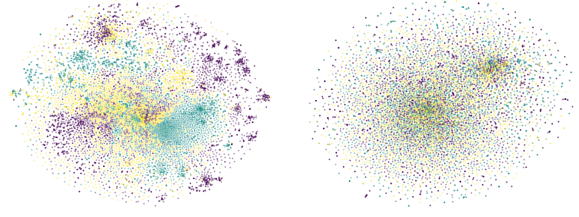


**Figure 2:** t-SNE visualization of GLOVE embeddings before (left) and after (right) erasure via Cascaded  $\bar{L}$ EOPARD with a rank-150 orthogonal projection. Gender is a ternary concept. Male-biased, female-biased, and neutral words are displayed in different colors.

from the [CLS] token. For DIAL, we use the representations from Basu Roy Chowdhury et al. (2023), obtained from a DeepMoji encoder [14] fine-tuned for sentiment classification.

All models are trained using the Adam optimizer [17]. For  $\bar{L}$ EOPARD, weight decay is set to zero to avoid interfering with the optimization of the projection loss (Eq. 3).

We set  $\gamma$  proportionally to  $\frac{1}{r^2}$  in the learning objective (Eq. 7). In Algorithm 1, we set  $U^{(0)} = (I_r \ 0)^T \in \mathbb{R}^{d \times r}$ , a truncated identity matrix. This initialization yields  $\mathcal{L}_p(U^{(0)}) = 0$ , and we intend to maintain proximity to an orthogonal projection during training.

Evaluation is conducted using scikit-learn’s MLPs [21] for both probing and downstream classification tasks. All reported accuracies are averaged over five independent runs to ensure robustness.

## 5 Results

### 5.1 Nonlinear Concept Erasure

$\bar{L}$ EOPARD enables effective erasure of information associated with a discrete concept, with the projector rank  $r$  serving as a tunable parameter that controls the strength of the erasure. Empirically, we observe that the difficulty of recovering the concept post-erasure increases steadily as the number of preserved dimensions decreases (see Figure 3, left panels). In Table 1, we exhibit configurations where  $\bar{L}$ EOPARD outperforms nonlinear erasure baselines in terms of MDL or probing accuracy which drops to near-random levels. Notably, in Table 1a, gender treated as a ternary concept during training and evaluation is almost fully erased, demonstrating the validity of  $\bar{L}$ EOPARD beyond binary settings. Qualitatively, the visualizations in figure 2 and in figures 6,7 in Supplementary Material D illustrate that concept class groups, which were previously distinguishable, become indistinguishable following erasure via  $\bar{L}$ EOPARD.

Results reported in the left panels of Figure 3 highlights the superior erasure capabilities of Cascaded  $\bar{L}$ EOPARD (Algorithm 2). For a fixed projection rank, the difficulty of recovering the concept post-erasure is consistently higher with Cascaded  $\bar{L}$ EOPARD compared to the standard training (Algorithm 1). For a given value of MDL, Cascaded  $\bar{L}$ EOPARD retains a larger number of dimensions in the feature space. This confirms our intuition that  $\bar{L}$ EOPARD trained in a standard way struggles with the removal of strong linear signals, which undermines nonlinear erasure performance. However, concept erasure is achieved with standard  $\bar{L}$ EOPARD at low rank. Both FaRM and KRaM, in their standard forms, perform well in terms of both linear and nonlinear erasure, suggesting that implementing them in a cascaded setup should not improve their performance, which we confirm experimentally (see Supplementary Material D).

<sup>1</sup> <https://github.com/EleutherAI/concept-erasure>

**Table 1:** Concept erasure evaluation. Accuracies are reported in % and MDL in kBits.

(a) Gender erasure in GLOVE embeddings.  $a_z^{\text{bin}}$  (resp.  $a_z^{\text{ter}}$ ) denotes the accuracy to predict the gender considered as binary (resp. ternary).

	$a_z^{\text{bin}} \downarrow$	MDL $\uparrow$	$a_z^{\text{ter}} \downarrow$	$A_{50\%} \uparrow$	WS-353 $\uparrow$
<i>original</i>	$100.0 \pm 0.0$	0.1	$100.0 \pm 0.0$	1.00	0.70
<i>random</i>	50.0	–	33.3	0.50	–
FaRM	<b>52.7 <math>\pm</math> 0.4</b>	25.3	<b>36.4 <math>\pm</math> 0.6</b>	0.67	0.57
KRaM	53.7 $\pm$ 0.4	27.9	<b>36.1 <math>\pm</math> 0.5</b>	0.62	0.58
<b>LEOPARD</b>					
standard, $r=75$	57.3 $\pm$ 0.6	26.2	39.7 $\pm$ 0.4	0.75	0.45
cascaded, $r=125$	<b>51.8 <math>\pm</math> 0.9</b>	<b>30.4</b>	<b>36.3 <math>\pm</math> 0.5</b>	<b>0.76</b>	<b>0.64</b>

(b) Gender erasure in BIAS IN BIOS.

	$a_z \downarrow$	MDL $\uparrow$	$a_y \uparrow$
<i>original</i>	$99.4 \pm 0.0$	2.7	$80.0 \pm 0.1$
<i>random</i>	53.5	–	33.5
FaRM	58.8 $\pm$ 0.2	<b>236.9</b>	55.6 $\pm$ 0.1
KRaM	56.4 $\pm$ 0.3	211.8	51.4 $\pm$ 0.1
<b>LEOPARD</b>			
standard, $r=10$	58.8 $\pm$ 0.7	193.4	53.4 $\pm$ 0.1
cascaded, $r=50$	<b>54.1 <math>\pm</math> 0.2</b>	193.5	54.1 $\pm$ 0.6
cascaded, $r=150$	55.9 $\pm$ 0.3	192.2	<b>65.5 <math>\pm</math> 0.5</b>

(c) Race erasure in DIAL.

	$a_z \downarrow$	MDL $\uparrow$	$a_y \uparrow$
<i>original</i>	$88.0 \pm 0.1$	136.2	$75.8 \pm 0.1$
<i>random</i>	50.0	–	33.3
FaRM	<b>53.7 <math>\pm</math> 0.8</b>	<b>335.8</b>	<b>73.9 <math>\pm</math> 0.3</b>
KRaM	<b>53.7 <math>\pm</math> 0.5</b>	330.3	<b>73.9 <math>\pm</math> 0.2</b>
<b>LEOPARD</b>			
standard, $r=15$	56.8 $\pm$ 0.2	311.3	67.4 $\pm$ 0.1
cascaded, $r=15$	57.2 $\pm$ 0.3	309.0	70.2 $\pm$ 0.1

## 5.2 Erasure vs. utility tradeoff

The right panels of Figure 3 highlight a consistent trade-off between concept erasure and the utility of post-erasure representations across all benchmark datasets, with optimal configurations located in the upper-right regions. The rank  $r$ , which controls the strength of erasure, modulates this trade-off. FaRM and KRaM achieve strong erasure but at the cost of substantial degradation in utility for gender, as evidenced by their positions in the upper-left regions of the left panels in Figures 3a and 3b.

The adjustable rank of LEOPARD offers flexibility in navigating this trade-off, enabling configurations that outperform baselines across several settings. Notably, on GLOVE embeddings, LEOPARD better preserves both local neighborhood structure and semantic content (Table 1a).

On BIAS IN BIOS, FaRM and KRaM outperform LEOPARD in terms of MDL-based erasure at the expense of downstream task performance. At low rank, LEOPARD achieves trade-offs between probing accuracy and downstream task accuracy comparable to baselines (e.g.,  $r = 10$  and  $r = 50$  for standard and cascaded training, respectively, in Table 1b). Figure 3b reveals that beyond a certain threshold, performance plateaus; further reducing  $r$  yields marginal gains in erasure while significantly harming utility. In such cases, LEOPARD (e.g., at  $r = 150$  with cascaded training) allows for a more satisfying balance between the reduction of the probing accuracy and downstream accuracy compared to baselines.

On DIAL, for race erasure, LEOPARD remains competitive without outperforming the baselines. Relying on linear projections in LEOPARD provides advantages in simplicity, interpretability, and parameter efficiency. However, such linear methods are inherently

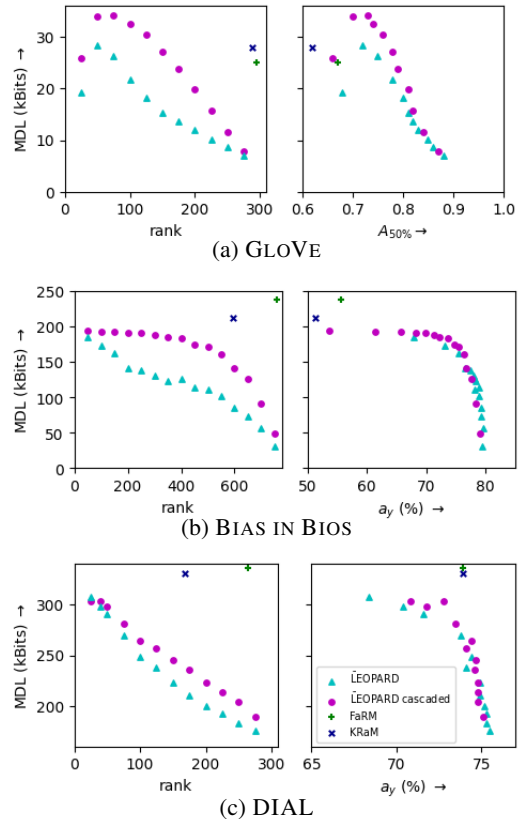


**Figure 3:** Erasure vs. rank of the feature space post-erasure (left) and Erasure–Utility trade-off (right) for each dataset. The vertical axis, erasure strength as evaluated by MDL, is shared between the right and left panels.

limited when addressing the erasure of concepts encoded nonlinearly. While erasing even a small number of dimensions can significantly reduce the recoverability of the target concept, achieving strong erasure often requires neutralizing a large subspace, which may degrade the utility of the resulting representations.

## 5.3 Fairness Analysis

Fairness evaluation results, reported in Table 2, demonstrate that LEOPARD significantly reduces gender and racial bias in downstream classification tasks, achieving performance comparable to the strongest baselines at low rank (e.g.,  $r = 10$  and  $r = 50$  with standard and cascaded training, respectively). The bias metrics consistently decrease as the number of preserved dimensions in the feature space is reduced, indicating an increasing level of bias mitigation.

Table 2a highlights a trade-off specific to the BIAS IN BIOS dataset between classifier performance on the downstream task (occupation prediction) and classifier fairness.<sup>2</sup> For FaRM and KRaM, achieving fairer classifiers comes at the cost of a substantial drop in downstream task accuracy. In contrast, the tunable rank in LEOPARD enables a more flexible compromise—for example, achieving significant gender bias reduction while incurring a smaller loss in downstream performance at  $r = 350$  or  $r = 250$  with Cascaded LEOPARD. The significant reduction of the positive correlation between the TPR gender gap for an occupation and the gender imbalance in that occupation at  $r = 250$  is made clearly visible in Figure 4.

<sup>2</sup> Such a trade-off has been demonstrated by Zaho & Gordon (2022)

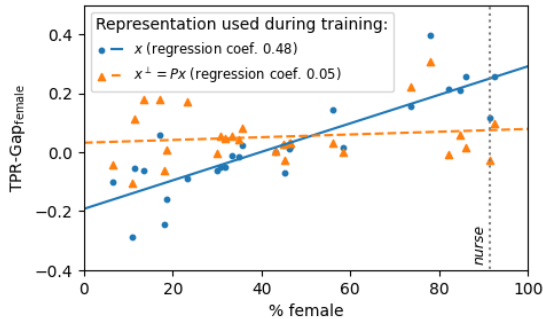
**Table 2:** Fairness evaluation of nonlinear downstream classifiers

(a) Occupation prediction on BIAS IN BIOS

	$a_y \uparrow$ (%)	$\text{GAP}_{\text{female}}^{\text{TPR,RMS}} \downarrow$	$\sigma_{\text{GAP},\% \text{female}} \downarrow$	$\text{DP} \downarrow$
<i>original</i>	$79.5 \pm 0.2$	$0.156 \pm 0.006$	$0.84 \pm 0.029$	$0.57 \pm 0.009$
FaRM	$55.6 \pm 0.1$	$0.073 \pm 0.004$	$0.31 \pm 0.021$	$0.33 \pm 0.004$
KRaM	$51.4 \pm 0.1$	<b><math>0.065 \pm 0.003</math></b>	<b><math>0.085 \pm 0.087</math></b>	<b><math>0.28 \pm 0.005</math></b>
<b><math>\bar{\text{LEOPARD}}</math></b>				
cascaded, $r=350$	<b><math>72.7 \pm 0.3</math></b>	$0.104 \pm 0.007$	$0.27 \pm 0.033$	$0.43 \pm 0.002$
cascaded, $r=250$	$70.1 \pm 0.4$	$0.106 \pm 0.004$	$0.13 \pm 0.050$	$0.40 \pm 0.006$
cascaded, $r=50$	$54.1 \pm 0.6$	$0.082 \pm 0.004$	<b><math>0.0079 \pm 0.075</math></b>	<b><math>0.29 \pm 0.007</math></b>
standard, $r=10$	$53.4 \pm 0.1$	<b><math>0.066 \pm 0.001</math></b>	<b><math>0.097 \pm 0.052</math></b>	$0.29 \pm 0.002$

(b) Sentiment prediction on DIAL

	$a_y \uparrow$ (%)	$\text{GAP}_{\text{AAE}}^{\text{TPR,RMS}} \downarrow$	$\text{DP} \downarrow$
<i>original</i>	$75.8 \pm 0.1$	$0.150 \pm 0.003$	$0.258 \pm 0.007$
FaRM	<b><math>73.9 \pm 0.3</math></b>	$0.071 \pm 0.005$	$0.060 \pm 0.005$
KRaM	<b><math>73.9 \pm 0.2</math></b>	$0.066 \pm 0.003$	$0.039 \pm 0.010$
<b><math>\bar{\text{LEOPARD}}</math></b>			
cascaded, $r=75$	<b><math>73.5 \pm 0.2</math></b>	$0.101 \pm 0.002$	$0.122 \pm 0.009$
cascaded, $r=50$	$71.8 \pm 0.2$	$0.069 \pm 0.004$	$0.071 \pm 0.005$
cascaded, $r=15$	$70.2 \pm 0.1$	<b><math>0.051 \pm 0.005</math></b>	$0.069 \pm 0.009$
standard, $r=15$	$67.4 \pm 0.1$	<b><math>0.042 \pm 0.004</math></b>	<b><math>0.022 \pm 0.003</math></b>

**Figure 4:** Average  $\text{TPR-Gap}_{\text{female},y}$  vs. female proportion in each occupation  $y$  for different representations used to train the classifiers.  $P$  is the rank-250 projection calculated via Cascaded  $\bar{\text{LEOPARD}}$ . Each vertical line corresponds to a specific occupation (e.g., nurse).

The results in Table 2b reveal a more nuanced picture: although  $\bar{\text{LEOPARD}}$  outperforms the baselines in bias reduction at low rank (e.g.  $r = 15$ ), it does so at the expense of lower downstream accuracy. Depending on the application context, particularly when fairness is a primary concern, the ability to adjust the rank makes  $\bar{\text{LEOPARD}}$  a favorable choice over less flexible methods.

#### 5.4 About MMD design choices

This work proposes an implementation of  $\bar{\text{LEOPARD}}$  designed for broad applicability with minimal hyperparameter tuning. As detailed in Section 4.2, several choices regarding the evaluation of MMD were informed by prior studies and supported by empirical evidence. Specifically, employing a single kernel ( $M = 1$ ) yields results of comparable magnitude to those reported in this article, while increasing  $M$  beyond 2 kernels yields only marginal improvements (see Supplementary Material F). We set  $M = 5$  in all experiments as a trade-off between performance and computational cost.

Regarding batch size, empirical analyses in Supplementary Material E indicate that large batches ( $b \geq 8192$ ) are preferable for gender erasure, while moderate batch sizes ( $b = 2048$ ) are well-suited for race erasure. Nevertheless, smaller batches ( $b = 512$ ) remain effective, often achieving competitive trade-offs and, in certain configurations, surpassing state-of-the-art baselines.

#### 5.5 About the freedom of choice for the rank

There is no universally optimal rank  $r$  for concept erasure with  $\bar{\text{LEOPARD}}$ . The ability to adjust the rank is a key strength of the method, allowing for context-specific trade-offs between erasure effectiveness and post-erasure representation utility. In practice, several strategies can guide the selection of an appropriate rank.

A straightforward approach involves defining a threshold on an erasure metric (e.g., MDL or validation accuracy), or more generally, on any task-independent criterion in unconstrained settings, and selecting the largest rank that satisfies this constraint. Alternatively, one may plot erasure and utility metrics as a function of  $r$ , similar to the analysis presented in Figure 3, to identify plateaus or local optima, providing a graphical heuristic for selecting a suitable rank.

## 6 Scope and Limitations

Our method specifically targets the erasure of discrete concepts. It could be naturally extended to the erasure of multiple discrete concepts by replacing the *erasure loss* (Eq. 6) with a sum of individual erasure losses, one per concept to be erased, in Eq. 7. With  $\bar{\text{LEOPARD}}$ , we do not address the erasure of continuous concepts, as the density matching objective in Eq. 6 requires partitioning samples according to discrete concept classes. For continuous concept erasure, approaches such as FaRM [3] or KRaM [4] are more suitable.

While our approach currently relies on orthogonal projections to ensure the preservation of local geometric structure and to avoid trivial solutions (e.g., constant mappings), this restriction limits the expressiveness of the method. Experiments on the DIAL dataset highlight this limitation: effective neutralization requires removing a large number of dimensions, which adversely impacts information preservation. To address this, future work will investigate integrating nonlinear erasure functions with the density matching objective.

## 7 Conclusion and future work

We introduced  $\bar{\text{LEOPARD}}$ , a simple yet effective method for nonlinear concept erasure which uses orthogonal projections to neutralize concept-specific information. By optimizing a density matching objective,  $\bar{\text{LEOPARD}}$  ensures indistinguishability of class-conditional distributions in the embedding space after erasure. Evaluated on classic NLP benchmarks,  $\bar{\text{LEOPARD}}$  is competitive and even outperforms state-of-the-art methods in nonlinear erasure of demographic attributes while better preserving the post-erasure utility of the representations. A notable strength of  $\bar{\text{LEOPARD}}$  is its ability to control the trade-off between concept erasure and information preservation by adjusting the rank of the learned projection. Empirical results also demonstrate that  $\bar{\text{LEOPARD}}$  improves fairness in downstream classifiers with a moderate impact on task performance.

Future research could explore applying the class-conditional density matching objective within an end-to-end model training alongside a generic objective such as MLM for BERT fine-tuning. Additionally, our approach could provide new insights into fairness and causal effect evaluation.

## References

- [1] E. D. Abraham, K. D'Oosterlinck, A. Feder, Y. Gat, A. Geiger, C. Potts, R. Reichart, and Z. Wu. CEBaB: Estimating the causal effects of real-world concepts on nlp model behavior. *Advances in Neural Information Processing Systems*, 35:17582–17596, 2022.
- [2] E. Agirre, E. Alfonseca, K. Hall, J. Kravalova, M. Paşca, and A. Soroa. A study on similarity and relatedness using distributional and WordNet-based approaches. In M. Ostendorf, M. Collins, S. Narayanan, D. W. Oard, and L. Vanderwende, editors, *Proceedings of Human Language Technologies: The 2009 Annual Conference of the North American Chapter of the Association for Computational Linguistics*, pages 19–27, Boulder, Colorado, June 2009. Association for Computational Linguistics.
- [3] S. Basu Roy Chowdhury and S. Chaturvedi. Learning fair representations via rate-distortion maximization. *Transactions of the Association for Computational Linguistics*, 10:1159–1174, 2022. doi: 10.1162/tacl\_a\_00512.
- [4] S. Basu Roy Chowdhury, N. Monath, K. A. Dubey, A. Ahmed, and S. Chaturvedi. Robust concept erasure via kernelized rate-distortion maximization. *Advances in Neural Information Processing Systems*, 36, 2023.
- [5] N. Belrose, D. Schneider-Joseph, S. Ravfogel, R. Cotterell, E. Raff, and S. Biderman. LEACE: Perfect linear concept erasure in closed form. In *Thirty-seventh Conference on Neural Information Processing Systems*, 2023.
- [6] S. L. Blodgett, L. Green, and B. O'Connor. Demographic dialectal variation in social media: A case study of african-american english. In *Proceedings of the 2016 Conference on Empirical Methods in Natural Language Processing*, pages 1119–1130, 2016.
- [7] T. Bolukbasi, K.-W. Chang, J. Y. Zou, V. Saligrama, and A. T. Kalai. Man is to computer programmer as woman is to homemaker? debiasing word embeddings. *Advances in neural information processing systems*, 29, 2016.
- [8] T. Brown, B. Mann, N. Ryder, M. Subbiah, J. D. Kaplan, P. Dhariwal, A. Neelakantan, P. Shyam, G. Sastry, A. Askell, S. Agarwal, A. Herbert-Voss, G. Krueger, T. Henighan, R. Child, A. Ramesh, D. Ziegler, J. Wu, C. Winter, C. Hesse, M. Chen, E. Sigler, M. Litwin, S. Gray, B. Chess, J. Clark, C. Berner, S. McCandlish, A. Radford, I. Sutskever, and D. Amodei. Language models are few-shot learners. In H. Larochelle, M. Ranzato, R. Hadsell, M. Balcan, and H. Lin, editors, *Advances in Neural Information Processing Systems*, volume 33, pages 1877–1901. Curran Associates, Inc., 2020.
- [9] A. Caliskan, J. J. Bryson, and A. Narayanan. Semantics derived automatically from language corpora contain human-like biases. *Science*, 356(6334):183–186, 2017. doi: 10.1126/science.aal4230.
- [10] M. De-Arteaga, A. Romanov, H. Wallach, J. Chayes, C. Borgs, A. Choudechova, S. Geyik, K. Kenthapadi, and A. T. Kalai. Bias in bios: A case study of semantic representation bias in a high-stakes setting. In *Proceedings of the Conference on Fairness, Accountability, and Transparency*, FAT\* '19, page 120–128, New York, NY, USA, 2019. Association for Computing Machinery. ISBN 9781450361255. doi: 10.1145/3287560.3287572.
- [11] J. Devlin, M.-W. Chang, K. Lee, and K. Toutanova. Bert: Pre-training of deep bidirectional transformers for language understanding. In *Proceedings of the 2019 Conference of the North American Chapter of the Association for Computational Linguistics: Human Language Technologies, NAACL-HLT 2019*, volume 1, pages 4171–4186, Minneapolis, MN, USA, 2019. Association for Computational Linguistics.
- [12] Y. Elazar and Y. Goldberg. Adversarial removal of demographic attributes from text data. In E. Riloff, D. Chiang, J. Hockenmaier, and J. Tsujii, editors, *Proceedings of the 2018 Conference on Empirical Methods in Natural Language Processing*, pages 11–21, Brussels, Belgium, Oct.-Nov. 2018. Association for Computational Linguistics. doi: 10.18653/v1/D18-1002.
- [13] A. Feder, N. Oved, U. Shalit, and R. Reichart. CausaLM: Causal model explanation through counterfactual language models. *Computational Linguistics*, 47(2):333–386, 2021.
- [14] B. Felbo, A. Misllove, A. Søgaard, I. Rahwan, and S. Lehmann. Using millions of emoji occurrences to learn any-domain representations for detecting sentiment, emotion and sarcasm. In *Proceedings of the 2017 Conference on Empirical Methods in Natural Language Processing*, pages 1615–1625, 2017.
- [15] Y. Ganin, E. Ustinova, H. Ajakan, P. Germain, H. Larochelle, F. Laviolette, M. March, and V. Lempitsky. Domain-adversarial training of neural networks. *Journal of machine learning research*, 17(59):1–35, 2016.
- [16] A. Gretton, K. M. Borgwardt, M. J. Rasch, B. Schölkopf, and A. Smola. A kernel two-sample test. *Journal of Machine Learning Research*, 13 (25):723–773, 2012.
- [17] D. P. Kingma and J. Ba. Adam: A method for stochastic optimization. In Y. Bengio and Y. LeCun, editors, *3rd International Conference on Learning Representations, ICLR 2015, San Diego, CA, USA, May 7-9, 2015. Conference Track Proceedings*, 2015.
- [18] P. Lemberger and A. Saillenfest. Explaining text classifiers with counterfactual representations. In U. Endriss, F. S. Melo, K. Bach, A. J. B. Diz, J. M. Alonso-Moral, S. Barro, and F. Heintz, editors, *ECAI 2024 - 27th European Conference on Artificial Intelligence, 19-24 October 2024, Santiago de Compostela, Spain - Including 13th Conference on Prestigious Applications of Intelligent Systems (PAIS 2024)*, volume 392 of *Frontiers in Artificial Intelligence and Applications*, pages 890–897. IOS Press, 2024. doi: 10.3233/FAIA240576.
- [19] Y. Li, K. Swersky, and R. Zemel. Generative moment matching networks. In F. Bach and D. Blei, editors, *Proceedings of the 32nd International Conference on Machine Learning*, volume 37 of *Proceedings of Machine Learning Research*, pages 1718–1727, Lille, France, 07–09 Jul 2015. PMLR.
- [20] M. Makar, B. Packer, D. Moldovan, D. Blalock, Y. Halpern, and A. D'Amour. Causally motivated shortcut removal using auxiliary labels. In *International Conference on Artificial Intelligence and Statistics*, pages 739–766. PMLR, 2022.
- [21] F. Pedregosa, G. Varoquaux, A. Gramfort, V. Michel, B. Thirion, O. Grisel, M. Blondel, P. Prettenhofer, R. Weiss, V. Dubourg, et al. Scikit-learn: Machine learning in python. *the Journal of machine Learning research*, 12:2825–2830, 2011.
- [22] J. Pennington, R. Socher, and C. D. Manning. Glove: Global vectors for word representation. In *Proceedings of the 2014 conference on empirical methods in natural language processing (EMNLP)*, pages 1532–1543, 2014.
- [23] S. Ravfogel, Y. Elazar, H. Gonen, M. Twiton, and Y. Goldberg. Null it out: Guarding protected attributes by iterative nullspace projection. In D. Jurafsky, J. Chai, N. Schluter, and J. Tetreault, editors, *Proceedings of the 58th Annual Meeting of the Association for Computational Linguistics*, pages 7237–7256, Online, July 2020. Association for Computational Linguistics. doi: 10.18653/v1/2020.acl-main.647.
- [24] S. Ravfogel, M. Twiton, Y. Goldberg, and R. D. Cotterell. Linear adversarial concept erasure. In *International Conference on Machine Learning*, pages 18400–18421. PMLR, 2022.
- [25] S. Ravfogel, F. Vargas, Y. Goldberg, and R. Cotterell. Adversarial concept erasure in kernel space. In *Proceedings of the 2022 Conference on Empirical Methods in Natural Language Processing*, pages 6034–6055, 2022.
- [26] S. Singh, S. Ravfogel, J. Herzig, R. Aharoni, R. Cotterell, and P. Kumaraguru. Representation surgery: theory and practice of affine steering. In *Proceedings of the 41st International Conference on Machine Learning*, pages 45663–45680, 2024.
- [27] F. Vargas and R. Cotterell. Exploring the linear subspace hypothesis in gender bias mitigation. In B. Webber, T. Cohn, Y. He, and Y. Liu, editors, *Proceedings of the 2020 Conference on Empirical Methods in Natural Language Processing (EMNLP)*, pages 2902–2913, Online, Nov. 2020. Association for Computational Linguistics. doi: 10.18653/v1/2020.emnlp-main.232.
- [28] V. Veitch, A. D'Amour, S. Yadlowsky, and J. Eisenstein. Counterfactual invariance to spurious correlations in text classification. *Advances in neural information processing systems*, 34:16196–16208, 2021.
- [29] E. Voita and I. Titov. Information-theoretic probing with minimum description length. In B. Webber, T. Cohn, Y. He, and Y. Liu, editors, *Proceedings of the 2020 Conference on Empirical Methods in Natural Language Processing (EMNLP)*, pages 183–196, Online, Nov. 2020. Association for Computational Linguistics. doi: 10.18653/v1/2020.emnlp-main.14.
- [30] H. Zhao and G. J. Gordon. Inherent tradeoffs in learning fair representations. *Journal of Machine Learning Research*, 23(57):1–26, 2022.

## Supplementary material

### A Impact Statement and Ethical Considerations

This work explores the removal of demographic attributes information from pre-trained representations, with potential applications in fairness. However, we caution that the method should not be seen as a definitive solution to bias in neural models. Its effectiveness depends on context, including the data and fairness metrics in use. The experiments are limited to a specific set of datasets, which may not capture all forms of implicit gender bias, meaning some biases may persist post-application. Additionally, the method is tailored to a particular technical definition of bias and may not be robust to other forms of bias or adversarial approaches. We encourage future research to address these limitations and further investigate its applicability.

### B Proof that $\mathcal{L}_p(U)$ is the distance to the closest projection to $UU^\top$

Let  $\hat{P} = UU^\top$  and  $P = U_r U_r^\top$  where  $U_r$  is the matrix of eigenvectors corresponding to the non-zero eigenvalues of  $\hat{P}$ .  $U_r^\top U_r = I_r$  and  $P$  is an orthogonal projection.

Since  $U_r$  is the matrix of eigenvectors corresponding to the non-zero eigenvalues of  $\hat{P}$ , we can express  $\hat{P}$  as:

$$\hat{P} = U_r \Lambda U_r^\top$$

where  $\Lambda$  is the diagonal matrix of eigenvalues of  $\hat{P}$ . Thus, we have:

$$\hat{P}P = U_r \Lambda U_r^\top U_r U_r^\top = U_r \Lambda U_r^\top = \hat{P}$$

Since both  $\hat{P}$  and  $P$  are symmetric semi-positive definite matrices, we move to the Frobenius norm of the difference between  $\hat{P}$  and  $P$ :

$$\|\hat{P} - P\|_F^2 = \text{Tr}((\hat{P} - P)^2)$$

Expanding the terms, we obtain:

$$\|\hat{P} - P\|_F^2 = \text{Tr}(\hat{P}^2) + \text{Tr}(P^2) - 2\text{Tr}(\hat{P}P)$$

**Term 1:**  $\text{Tr}(\hat{P}^2)$

Since  $\hat{P} = UU^\top$ , we can use the property  $\|AB\|_F^2 = \|BA\|_F^2$  to write:

$$\text{Tr}(\hat{P}^2) = \|U^\top U\|_F^2$$

**Term 2:**  $\text{Tr}(P^2)$

Since  $P^2 = P$  (as  $P$  is an orthogonal projection matrix), and  $\text{rank}(P) = r$ , we have:

$$\text{Tr}(P^2) = \text{Tr}(P) = r = \|I_r\|_F^2$$

**Term 3:**  $\text{Tr}(\hat{P}P)$

From the equation  $\hat{P}P = \hat{P}$ , we conclude that:

$$\text{Tr}(\hat{P}P) = \text{Tr}(\hat{P}) = \text{Tr}(U^\top U)$$

**Final Expression**

Now substituting these results into the expression for the Frobenius norm:

$$\|\hat{P} - P\|_F^2 = \|U^\top U\|_F^2 + \|I_r\|_F^2 - 2\text{Tr}(U^\top U)$$

This simplifies to:

$$\|\hat{P} - P\|_F^2 = \|U^\top U - I_r\|_F^2$$

Finally, using Equation 3:

$$\|\hat{P} - P\|_F^2 = \mathcal{L}_p(U)$$

This completes the proof.

## C Training Details

### Hardware and Environment

All experiments are conducted on an NVIDIA GeForce RTX 2080 Ti GPU with 11GB of VRAM and an Intel(R) Core(TM) i9-9900K CPU, using PyTorch 2.0.1 and Python 3.11.4. We employ CUDA 12.6 for accelerated computations.

### Optimization and Hyperparameters for $\bar{\text{LEOPARD}}$

We use the Adam optimizer [17] with the following hyperparameters:

- Learning rate:  $1 \times 10^{-3}$  for GLOVE embeddings,  $5 \times 10^{-4}$  for BIAS IN BIOS and DIAL.
- Batch size: Full batch (10,777) for GLOVE embeddings, batches of size 8192 for BIAS IN BIOS, batches of size 2048 for DIAL.
- Weight decay: 0.0 (to avoid interfering with the *projection loss* (Eq. 3)).

Each training terminates after a fixed number of epochs ( $N_e = 1000$  for GLOVE embeddings,  $N_e = 100$  for BIAS IN BIOS,  $N_e = 200$  for DIAL). To improve convergence, we apply a learning rate scheduler that reduces the learning rate by a factor of 10 after  $\frac{N_e}{2}$  epochs.

### Model-Specific Settings

- $\bar{\text{LEOPARD}}$ :  $\gamma$  is scaled as  $\frac{1}{r^2}$ , using  $\frac{200}{r^2}$  for GLOVE embeddings and  $\frac{100}{r^2}$  for BIAS IN BIOS and Dial.
- **LEACE**: We relied on the publicly available implementation from <https://github.com/EleutherAI/concept-erasure>.
- **KRaM** and **FaRM**: We reimplemented KRaM [4] and FaRM [3]. We set  $\lambda = 0.7$  in KRaM’s loss. For GLOVE and BIAS IN BIOS, the erasure function results from training a 4-layer MLP. For Dial, the erasure map is a 7-layer MLP.

### Evaluation Metrics

Probing classifiers and downstream task models have been trained using `skikit-learn`’s `MLPClassifier` with the following settings:

- Learning rate:  $10^{-4}$  for the probes and the downstream classifiers.
- Max iterations: 20 for the probes and the downstream classifiers.
- Batch size: 512 for the probes and the downstream classifiers.

All reported accuracy and fairness metrics are averaged over five independent runs to ensure robustness.

MDL is evaluated on the full training set for GLOVE and DIAL and on a subset of 100k samples for BIAS IN BIOS.

## D Supplementary results

### D.1 GLOVE

**Table 3:** Gender erasure in GLOVE embeddings. ‡ denotes results reported from [3] and [4].

	$a_z^{\text{bin}} \downarrow$ (%)	MDL $\uparrow$ (kBits)	$a_z^{\text{ter}} \downarrow$ (%)	$A_{50\%} \uparrow$	WS-353 $\uparrow$	Rank
<i>original</i>	$100.0 \pm 0.0$	<i>0.1</i>	$100.0 \pm 0.0$	<i>1.00</i>	<i>0.70</i>	<i>300</i>
<i>random</i>	<i>50.0</i>	–	<i>33.3</i>	<i>0.50</i>	–	<i>300</i>
FaRM‡	53.9	24.6	–	0.65	–	247
KRaM‡	52.6	–	–	0.65	0.48	246
LEACE	$96.3 \pm 0.1$	3.5	$81.1 \pm 0.5$	0.94	0.69	298
FaRM	$52.7 \pm 0.4$	25.3	$36.4 \pm 0.6$	0.67	0.57	295
FaRM cascaded	$54.0 \pm 0.6$	25.0	$37.2 \pm 0.8$	0.66	0.56	297
KRaM	$53.7 \pm 0.4$	27.9	$36.1 \pm 0.5$	0.62	0.58	289
KRaM cascaded	$53.1 \pm 0.6$	27.8	$37.1 \pm 0.6$	0.64	0.56	288
<b><math>\bar{\text{LEOPARD}}</math> (standard)</b>						
$r = 275$	$88.8 \pm 0.5$	7.1	$70.0 \pm 0.4$	0.88	0.72	275
$r = 250$	$85.5 \pm 0.3$	8.7	$65.5 \pm 0.6$	0.86	0.69	250
$r = 225$	$82.1 \pm 0.5$	10.2	$60.9 \pm 0.6$	0.85	0.66	225
$r = 200$	$77.5 \pm 0.5$	12.0	$56.6 \pm 0.4$	0.83	0.65	200
$r = 175$	$74.0 \pm 0.9$	13.6	$53.3 \pm 0.6$	0.82	0.62	175
$r = 150$	$70.3 \pm 0.5$	15.3	$49.7 \pm 1.2$	0.81	0.58	150
$r = 125$	$65.6 \pm 0.5$	18.3	$46.2 \pm 0.5$	0.80	0.54	125
$r = 100$	$61.4 \pm 0.7$	21.7	$42.7 \pm 0.7$	0.78	0.48	100
$r = 75$	$57.3 \pm 0.6$	26.2	$39.7 \pm 0.4$	0.75	0.45	75
$r = 50$	$54.1 \pm 0.8$	28.3	$37.0 \pm 0.7$	0.72	0.34	50
$r = 25$	$51.1 \pm 0.8$	19.3	$35.4 \pm 0.8$	0.68	0.24	25
<b><math>\bar{\text{LEOPARD}}</math> (cascaded)</b>						
$r = 275$	$87.3 \pm 0.4$	8.0	$68.1 \pm 0.7$	0.87	0.73	275
$r = 250$	$80.6 \pm 0.2$	11.6	$60.2 \pm 0.6$	0.84	0.68	250
$r = 225$	$71.4 \pm 0.8$	15.7	$51.0 \pm 0.5$	0.82	0.65	225
$r = 200$	$65.2 \pm 0.7$	19.8	$45.4 \pm 0.7$	0.81	0.64	200
$r = 175$	$58.9 \pm 0.4$	23.8	$41.6 \pm 0.3$	0.79	0.63	175
$r = 150$	$55.9 \pm 1.1$	27.1	$38.1 \pm 0.6$	0.78	0.64	150
$r = 125$	$51.8 \pm 0.9$	30.4	$36.3 \pm 0.5$	0.76	0.64	125
$r = 100$	$51.0 \pm 0.4$	32.4	$35.4 \pm 0.7$	0.74	0.64	100
$r = 75$	$50.7 \pm 0.7$	34.1	$34.2 \pm 0.7$	0.73	0.60	75
$r = 50$	$50.4 \pm 0.6$	34.0	$34.3 \pm 1.0$	0.70	0.60	50
$r = 25$	$50.1 \pm 0.9$	25.9	$34.2 \pm 0.8$	0.66	0.49	25

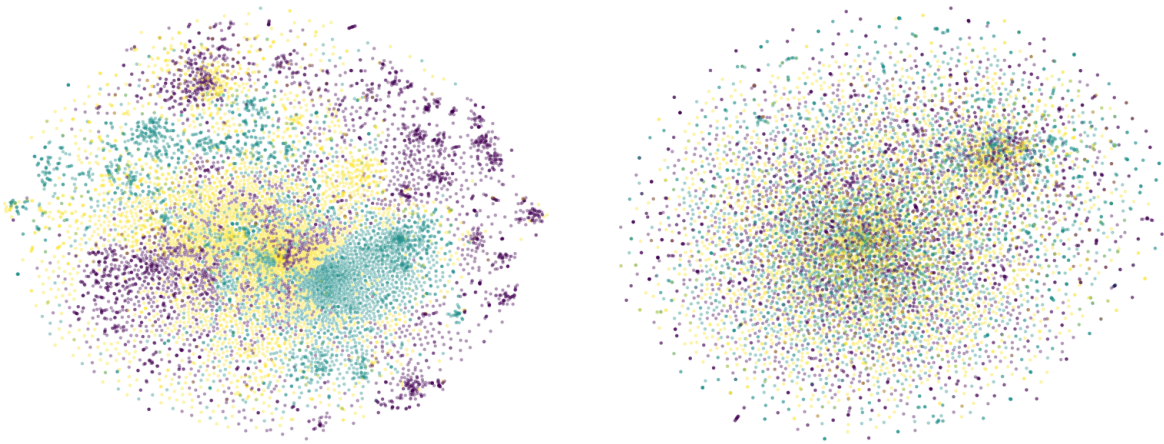


**Figure 5:** t-SNE visualization of GLOVE embeddings before erasure (left) and after erasure via  $\bar{\text{LEOPARD}}$  with a rank-150 orthogonal projection (right). Male-biased, female-biased, and neutral words are displayed in different colors.

## D.2 BIAS IN BIOS

**Table 4:** Gender erasure in BIAS IN BIOS. ‡ denotes results reported from [3] and [4].

	$a_z \downarrow$ (%)	MDL	$a_y \uparrow$ (%)	Rank
<i>original</i>	$99.4 \pm 0.0$	2.7	$80.0 \pm 0.1$	768
<i>random</i>	53.5	–	33.5	768
FaRM‡	55.6	–	55.8	–
LEACE	$98.6 \pm 0.1$	15.7	$79.8 \pm 0.2$	767
FaRM	$58.8 \pm 0.2$	236.9	$55.6 \pm 0.1$	759
FaRM cascaded	$58.0 \pm 0.4$	238.7	$54.6 \pm 0.2$	–
KRaM	$56.4 \pm 0.4$	211.8	$51.4 \pm 0.1$	593
KRaM cascaded	$56.2 \pm 0.5$	211.4	$51.8 \pm 0.2$	–
<b>LEOPARD</b>				
$r = 750$	$98.4 \pm 0.1$	31.0	$79.6 \pm 0.2$	750
$r = 700$	$97.0 \pm 0.9$	55.7	$79.5 \pm 0.2$	700
$r = 650$	$96.7 \pm 0.4$	77.4	$79.4 \pm 0.2$	650
$r = 600$	$95.6 \pm 0.2$	90.9	$79.1 \pm 0.3$	600
$r = 550$	$94.3 \pm 1.0$	97.5	$79.0 \pm 0.2$	550
$r = 500$	$93.4 \pm 0.8$	112.0	$78.9 \pm 0.1$	500
$r = 450$	$92.8 \pm 0.6$	110.7	$78.6 \pm 0.4$	450
$r = 400$	$91.6 \pm 0.8$	119.1	$78.4 \pm 0.3$	400
$r = 350$	$90.1 \pm 0.8$	126.4	$78.2 \pm 0.1$	350
$r = 300$	$88.9 \pm 0.3$	128.3	$77.9 \pm 0.1$	300
$r = 250$	$88.2 \pm 0.6$	133.8	$77.4 \pm 0.2$	250
$r = 200$	$85.7 \pm 0.4$	142.3	$76.8 \pm 0.1$	200
$r = 150$	$82.1 \pm 0.4$	158.7	$75.5 \pm 0.2$	150
$r = 100$	$77.1 \pm 0.7$	172.0	$73.2 \pm 0.2$	100
$r = 50$	$69.0 \pm 0.7$	186.2	$67.9 \pm 0.2$	50
$r = 10$	$58.8 \pm 0.7$	193.4	$53.4 \pm 0.1$	10
<b>LEOPARD (cascaded)</b>				
$r = 750$	$97.1 \pm 0.2$	48.7	$79.1 \pm 0.2$	750
$r = 700$	$93.7 \pm 0.4$	95.7	$78.5 \pm 0.2$	700
$r = 650$	$90.6 \pm 0.4$	126.7	$77.6 \pm 0.1$	650
$r = 600$	$86.3 \pm 1.2$	147.3	$76.7 \pm 0.1$	600
$r = 550$	$82.8 \pm 1.7$	160.7	$76.2 \pm 0.2$	550
$r = 500$	$79.7 \pm 1.5$	171.5	$75.5 \pm 0.1$	500
$r = 450$	$76.2 \pm 1.8$	176.0	$74.7 \pm 0.2$	450
$r = 400$	$72.6 \pm 2.6$	182.2	$73.7 \pm 0.3$	400
$r = 350$	$67.4 \pm 2.0$	185.5	$72.7 \pm 0.3$	350
$r = 300$	$63.1 \pm 1.4$	189.8	$71.7 \pm 0.4$	300
$r = 250$	$59.7 \pm 0.6$	190.8	$70.1 \pm 0.4$	250
$r = 200$	$57.3 \pm 0.9$	191.2	$68.1 \pm 0.6$	200
$r = 150$	$55.9 \pm 0.3$	192.2	$65.5 \pm 0.5$	150
$r = 100$	$55.1 \pm 0.3$	193.1	$61.5 \pm 0.6$	100
$r = 50$	$54.1 \pm 0.2$	193.5	$54.1 \pm 0.6$	50



**Figure 6:** t-SNE visualization of BIAS IN BIOS embeddings before erasure (left) and after erasure via cascaded LEOPARD with a rank-250 orthogonal projection (right). Female-biased and male-biased text representations are displayed in different colors.

### D.3 DIAL

**Table 5:** Race erasure in DIAL. ‡ denotes results reported from [3] and [4].

	$a_z \downarrow$	MDL $\uparrow$	$a_y \uparrow$	DP $\downarrow$	rank
<i>original</i>	$88.0 \pm 0.1$	136.2	$75.8 \pm 0.1$	0.26	300
<i>random</i>	50.0		33.3	–	300
FaRM‡	54.2	–	74.8	0.09	–
KRaM‡	54.0	–	72.4	0.08	–
LEACE	$84.5 \pm 0.5$	190.0	$75.7 \pm 0.1$	0.17	299
FaRM	$53.7 \pm 0.8$	335.8	$73.9 \pm 0.3$	0.06	264
FaRM (cascaded)	$54.2 \pm 0.4$	343.8	$66.9 \pm 0.3$	0.03	248
KRaM	$53.7 \pm 0.5$	330.3	$73.9 \pm 0.2$	0.04	168
KRaM (cascaded)	$53.0 \pm 0.2$	324.4	$65.8 \pm 0.1$	0.04	215
<b>LEOPARD</b>					
$r = 275$	$86.3 \pm 0.2$	176.0	$75.5 \pm 0.2$	0.19	275
$r = 250$	$86.0 \pm 0.3$	183.1	$75.3 \pm 0.2$	0.21	250
$r = 225$	$85.4 \pm 0.2$	193.1	$75.3 \pm 0.1$	0.21	225
$r = 200$	$84.8 \pm 0.2$	200.6	$75.2 \pm 0.2$	0.18	200
$r = 175$	$83.8 \pm 0.4$	210.7	$74.9 \pm 0.3$	0.17	175
$r = 150$	$82.8 \pm 0.2$	223.4	$74.9 \pm 0.1$	0.17	150
$r = 125$	$80.9 \pm 0.3$	238.6	$74.1 \pm 0.2$	0.15	125
$r = 100$	$78.9 \pm 0.5$	248.3	$74.4 \pm 0.1$	0.18	100
$r = 75$	$75.8 \pm 0.3$	269.3	$73.8 \pm 0.2$	0.13	75
$r = 50$	$70.2 \pm 0.7$	290.7	$71.6 \pm 0.2$	0.13	50
$r = 40$	$67.8 \pm 0.2$	298.3	$70.4 \pm 0.2$	0.09	40
$r = 25$	$61.1 \pm 0.4$	307.9	$68.4 \pm 0.1$	0.04	25
$r = 15$	$56.8 \pm 0.2$	311.3	$67.4 \pm 0.1$	0.02	15
<b>LEOPARD cascaded</b>					
$r = 275$	$85.5 \pm 0.2$	189.6	$75.1 \pm 0.1$	0.17	275
$r = 250$	$84.5 \pm 0.3$	204.1	$74.8 \pm 0.2$	0.16	250
$r = 225$	$83.8 \pm 0.3$	213.7	$74.8 \pm 0.1$	0.15	225
$r = 200$	$83.1 \pm 0.2$	223.9	$74.8 \pm 0.1$	0.15	200
$r = 175$	$81.3 \pm 0.2$	236.0	$74.6 \pm 0.3$	0.13	175
$r = 150$	$80.4 \pm 0.4$	245.0	$74.7 \pm 0.2$	0.13	150
$r = 125$	$78.5 \pm 0.2$	257.0	$74.1 \pm 0.2$	0.14	125
$r = 100$	$77.4 \pm 0.3$	264.1	$74.4 \pm 0.2$	0.14	100
$r = 75$	$73.3 \pm 0.4$	281.5	$73.5 \pm 0.2$	0.12	75
$r = 50$	$67.6 \pm 0.3$	297.6	$71.8 \pm 0.2$	0.08	50
$r = 40$	$64.5 \pm 0.4$	303.3	$70.8 \pm 0.4$	0.07	40
$r = 25$	$62.4 \pm 0.3$	303.0	$72.8 \pm 0.2$	0.11	25
$r = 15$	$57.2 \pm 0.3$	309.0	$70.2 \pm 0.1$	0.07	15

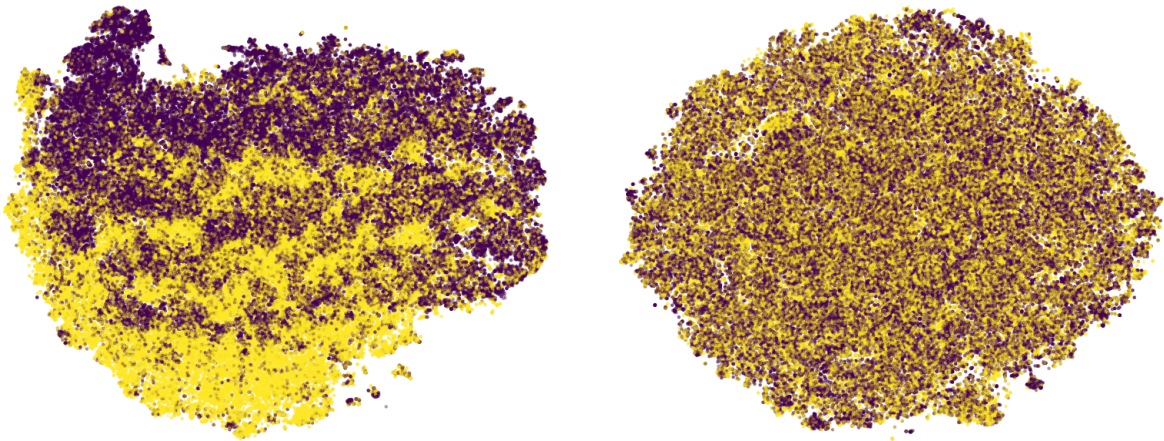


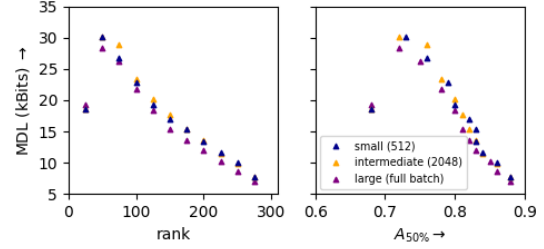
**Figure 7:** t-SNE visualization of DIAL embeddings before erasure (left) and after erasure via cascaded LEOPARD with a rank-50 orthogonal projection (right). Representations of tweets written in *African-American English* and *Standard American English* are displayed in different colors.

## E Batch size analysis

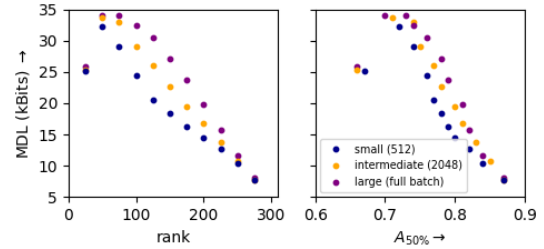
### E.1 GLOVE

**Table 6:** Gender erasure in GLOVE with  $\bar{\text{LEOPARD}}$  for different batch sizes used during training.

	rank	$a_{\text{er}}^{\text{bin}} \downarrow$ (%)	MDL $\uparrow$ (kBits)	$a_{\text{er}}^{\text{er}} \downarrow$ (%)	$A_{50\%} \uparrow$	WS-353 $\uparrow$
$\bar{\text{LEOPARD}}$						
$r = 275$	full batch	88.8 $\pm$ 0.5	7.1	70.0 $\pm$ 0.4	0.88	0.72
	2048	88.0 $\pm$ 0.2	7.7	68.9 $\pm$ 0.9	0.88	0.73
	512	87.5 $\pm$ 0.1	7.7	68.2 $\pm$ 0.7	0.88	0.71
$r = 250$	full batch	85.5 $\pm$ 0.3	8.7	65.5 $\pm$ 0.6	0.86	0.69
	2048	83.8 $\pm$ 0.2	9.8	63.0 $\pm$ 0.7	0.86	0.69
	512	83.3 $\pm$ 0.8	10.0	62.2 $\pm$ 0.1	0.86	0.67
$r = 225$	full batch	82.1 $\pm$ 0.5	10.2	60.9 $\pm$ 0.6	0.85	0.66
	2048	78.5 $\pm$ 0.8	11.5	58.1 $\pm$ 0.6	0.84	0.66
	512	78.3 $\pm$ 0.5	11.7	57.2 $\pm$ 0.4	0.84	0.65
$r = 200$	full batch	77.5 $\pm$ 0.5	12.0	56.6 $\pm$ 0.4	0.83	0.65
	2048	74.3 $\pm$ 0.3	13.5	54.3 $\pm$ 0.6	0.83	0.63
	512	74.8 $\pm$ 0.4	13.4	54.0 $\pm$ 0.7	0.83	0.63
$r = 175$	full batch	74.0 $\pm$ 0.9	13.6	53.3 $\pm$ 0.6	0.82	0.62
	2048	71.2 $\pm$ 0.6	15.4	50.3 $\pm$ 0.2	0.82	0.60
	512	71.6 $\pm$ 0.5	15.4	50.3 $\pm$ 1.1	0.83	0.61
$r = 150$	full batch	70.3 $\pm$ 0.5	15.3	49.7 $\pm$ 1.2	0.81	0.58
	2048	66.6 $\pm$ 0.4	17.7	47.1 $\pm$ 0.4	0.81	0.57
	512	68.1 $\pm$ 0.7	17.0	47.8 $\pm$ 0.7	0.82	0.58
$r = 125$	full batch	65.6 $\pm$ 0.5	18.3	46.2 $\pm$ 0.5	0.80	0.54
	2048	62.4 $\pm$ 0.5	20.1	44.1 $\pm$ 0.5	0.80	0.54
	512	65.5 $\pm$ 0.3	19.2	44.8 $\pm$ 0.7	0.80	0.57
$r = 100$	full batch	61.4 $\pm$ 0.7	21.7	42.7 $\pm$ 0.7	0.78	0.48
	2048	59.5 $\pm$ 0.8	23.4	40.0 $\pm$ 0.6	0.78	0.47
	512	61.2 $\pm$ 0.9	22.8	42.3 $\pm$ 0.7	0.79	0.52
$r = 75$	full batch	57.3 $\pm$ 0.6	26.2	39.7 $\pm$ 0.4	0.75	0.45
	2048	54.9 $\pm$ 0.5	28.9	37.9 $\pm$ 0.5	0.76	0.43
	512	56.1 $\pm$ 0.8	26.7	38.9 $\pm$ 0.8	0.76	0.48
$r = 50$	full batch	54.1 $\pm$ 0.8	28.3	37.0 $\pm$ 0.7	0.72	0.34
	2048	52.5 $\pm$ 1.2	30.1	35.7 $\pm$ 0.3	0.72	0.36
	512	53.1 $\pm$ 0.5	30.1	36.4 $\pm$ 0.4	0.73	0.37
$r = 25$	full batch	51.1 $\pm$ 0.8	19.3	35.4 $\pm$ 0.8	0.68	0.24
	2048	50.9 $\pm$ 0.7	18.6	34.5 $\pm$ 1.0	0.68	0.27
	512	51.3 $\pm$ 1.1	18.6	34.8 $\pm$ 1.2	0.68	0.27
$\bar{\text{LEOPARD}}$ (cascaded)						
$r = 275$	full batch	87.3 $\pm$ 0.4	8.0	68.1 $\pm$ 0.7	0.87	0.73
	2048	87.7 $\pm$ 0.5	7.8	68.5 $\pm$ 0.5	0.87	0.73
	512	87.7 $\pm$ 0.3	7.8	68.6 $\pm$ 0.2	0.87	0.74
$r = 250$	full batch	80.6 $\pm$ 0.2	11.6	60.2 $\pm$ 0.6	0.84	0.68
	2048	81.6 $\pm$ 0.4	10.8	60.7 $\pm$ 0.5	0.85	0.69
	512	82.3 $\pm$ 0.4	10.3	62.1 $\pm$ 0.3	0.84	0.73
$r = 225$	full batch	71.4 $\pm$ 0.8	15.7	51.0 $\pm$ 0.5	0.82	0.65
	2048	74.6 $\pm$ 0.7	13.8	53.6 $\pm$ 0.9	0.83	0.68
	512	77.4 $\pm$ 0.2	12.7	56.2 $\pm$ 0.6	0.82	0.71
$r = 200$	full batch	65.2 $\pm$ 0.7	19.8	45.4 $\pm$ 0.7	0.81	0.64
	2048	69.8 $\pm$ 1.2	16.8	49.1 $\pm$ 1.1	0.81	0.68
	512	72.8 $\pm$ 0.7	14.4	51.5 $\pm$ 0.8	0.80	0.71
$r = 175$	full batch	58.9 $\pm$ 0.4	23.8	41.6 $\pm$ 0.3	0.79	0.63
	2048	64.5 $\pm$ 0.3	19.4	44.7 $\pm$ 0.5	0.80	0.67
	512	68.4 $\pm$ 0.8	16.2	47.6 $\pm$ 0.6	0.79	0.71
$r = 150$	full batch	55.9 $\pm$ 1.1	27.1	38.1 $\pm$ 0.6	0.78	0.64
	2048	60.5 $\pm$ 0.6	22.7	42.1 $\pm$ 0.5	0.78	0.66
	512	65.7 $\pm$ 0.4	18.4	45.5 $\pm$ 0.6	0.78	0.69
$r = 125$	full batch	51.8 $\pm$ 0.9	30.4	36.3 $\pm$ 0.5	0.76	0.64
	2048	57.2 $\pm$ 0.6	26.1	39.3 $\pm$ 1.0	0.77	0.65
	512	62.5 $\pm$ 0.8	20.6	43.4 $\pm$ 0.9	0.77	0.67
$r = 100$	full batch	51.0 $\pm$ 0.4	32.4	35.4 $\pm$ 0.7	0.74	0.64
	2048	54.5 $\pm$ 0.2	29.1	37.1 $\pm$ 0.3	0.75	0.63
	512	59.8 $\pm$ 1.0	24.4	40.8 $\pm$ 0.5	0.76	0.63
$r = 75$	full batch	50.7 $\pm$ 0.7	34.1	34.2 $\pm$ 0.7	0.73	0.60
	2048	53.1 $\pm$ 0.7	33.0	35.4 $\pm$ 0.9	0.74	0.60
	512	57.0 $\pm$ 0.6	29.0	38.0 $\pm$ 0.6	0.74	0.58
$r = 50$	full batch	50.4 $\pm$ 0.6	34.0	34.3 $\pm$ 1.0	0.70	0.60
	2048	51.2 $\pm$ 0.3	33.7	34.5 $\pm$ 0.9	0.71	0.59
	512	53.5 $\pm$ 0.6	32.2	36.2 $\pm$ 0.7	0.72	0.52
$r = 25$	full batch	50.1 $\pm$ 0.9	25.9	34.2 $\pm$ 0.8	0.66	0.49
	2048	50.8 $\pm$ 0.7	25.3	34.4 $\pm$ 0.6	0.66	0.49
	512	52.2 $\pm$ 0.8	25.2	35.2 $\pm$ 0.5	0.67	0.44



(a) Standard training



(b) Cascaded training

**Figure 8:** Gender erasure in GLOVE with  $\bar{\text{LEOPARD}}$  vs. rank of the feature space post-erasure (left) and Erasure–Utility trade-off (right) for different batch sizes used during training. The vertical axis, erasure strength as evaluated by MDL, is shared between the right and left panels.

## E.2 BIAS IN BIOS

In order to limit computation costs, we have restricted the analysis to a reduced number of  $r$  values.

**Table 7:** Gender erasure in BIAS IN BIOS with  $\overline{\text{LEOPARD}}$  for different batch sizes used during training.

	batch size	$a_z \downarrow$ (%)	MDL	$a_y \uparrow$ (%)
$\overline{\text{LEOPARD}}$				
$r = 200$	8192	$85.7 \pm 0.4$	142.3	$76.8 \pm 0.1$
	2048	$83.5 \pm 0.8$	151.4	$77.1 \pm 0.2$
	512	$83.7 \pm 0.4$	146.0	$77.5 \pm 0.2$
$r = 150$	8192	$82.1 \pm 0.4$	158.7	$75.5 \pm 0.2$
	2048	$80.0 \pm 0.4$	164.5	$76.3 \pm 0.1$
	512	$80.6 \pm 0.3$	159.3	$77.1 \pm 0.1$
$r = 100$	8192	$77.1 \pm 0.7$	172.0	$73.2 \pm 0.2$
	2048	$75.6 \pm 0.4$	175.1	$74.3 \pm 0.3$
	512	$76.3 \pm 0.5$	169.7	$75.9 \pm 0.3$
$r = 50$	8192	$69.0 \pm 0.7$	186.2	$67.9 \pm 0.2$
	2048	$67.9 \pm 0.4$	186.4	$70.1 \pm 0.1$
	512	$69.9 \pm 0.2$	183.8	$72.6 \pm 0.2$
$\overline{\text{LEOPARD}}$ (cascaded)				
$r = 200$	8192	$57.3 \pm 0.9$	191.2	$68.1 \pm 0.6$
	2048	$61.4 \pm 1.1$	189.0	$70.1 \pm 0.4$
	512	$65.3 \pm 0.0$	187.7	$70.7 \pm 0.4$
$r = 150$	8192	$55.9 \pm 0.3$	192.2	$65.5 \pm 0.5$
	2048	$59.8 \pm 1.1$	189.9	$68.1 \pm 0.3$
	512	$63.8 \pm 1.5$	188.7	$69.1 \pm 0.2$
$r = 100$	8192	$55.1 \pm 0.3$	193.1	$61.5 \pm 0.6$
	2048	$57.5 \pm 0.3$	190.9	$64.6 \pm 0.3$
	512	$62.1 \pm 0.5$	187.9	$66.7 \pm 0.3$
$r = 50$	8192	$54.1 \pm 0.2$	193.5	$54.1 \pm 0.6$
	2048	$54.9 \pm 0.4$	192.2	$58.3 \pm 0.4$
	512	$58.2 \pm 0.6$	190.9	$62.2 \pm 0.3$

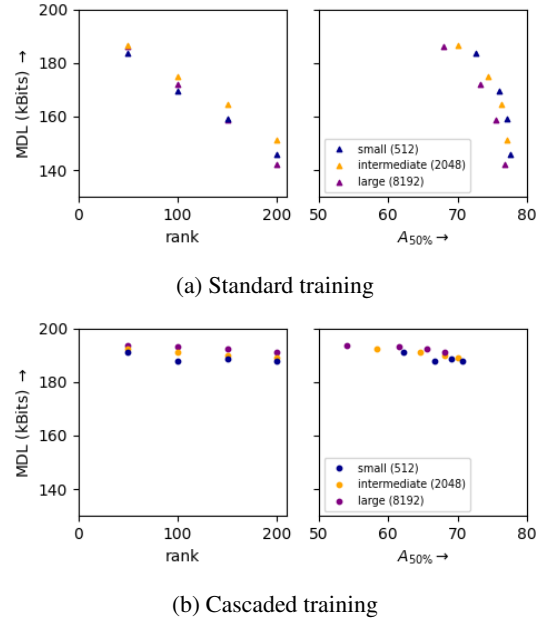


**Figure 9:** Gender erasure in BIAS IN BIOS with  $\overline{\text{LEOPARD}}$  vs. rank of the feature space post-erasure (left) and Erasure-Utility trade-off (right) for different batch sizes used during training. The vertical axis, erasure strength as evaluated by MDL, is shared between the right and left panels.

### E.3 DIAL

**Table 8:** Race erasure in DIAL with  $\bar{\text{LEOPARD}}$  for different batch sizes used during training.

	batch size	$a_z \downarrow$	MDL $\uparrow$	$a_y \uparrow$	DP $\downarrow$
$\bar{\text{LEOPARD}}$ (standard)					
$r = 275$	8192	86.5 $\pm$ 0.2	172.7	75.7 $\pm$ 0.1	0.19
	2048	86.3 $\pm$ 0.2	176.0	75.5 $\pm$ 0.2	0.19
	512	86.0 $\pm$ 0.2	174.7	75.7 $\pm$ 0.1	0.19
$r = 250$	8192	86.1 $\pm$ 0.2	180.0	75.0 $\pm$ 0.1	0.20
	2048	86.0 $\pm$ 0.3	183.1	75.3 $\pm$ 0.2	0.21
	512	85.7 $\pm$ 0.3	180.6	75.4 $\pm$ 0.2	0.18
$r = 225$	8192	85.8 $\pm$ 0.1	188.5	74.8 $\pm$ 0.2	0.19
	2048	85.4 $\pm$ 0.2	193.1	75.3 $\pm$ 0.1	0.21
	512	85.2 $\pm$ 0.1	190.5	75.4 $\pm$ 0.2	0.19
$r = 200$	8192	85.3 $\pm$ 0.1	194.7	74.8 $\pm$ 0.3	0.17
	2048	84.8 $\pm$ 0.2	200.6	75.2 $\pm$ 0.2	0.18
	512	84.4 $\pm$ 0.2	197.1	75.3 $\pm$ 0.2	0.18
$r = 175$	8192	84.7 $\pm$ 0.3	205.0	74.6 $\pm$ 0.3	0.16
	2048	83.8 $\pm$ 0.4	210.7	74.9 $\pm$ 0.3	0.17
	512	83.5 $\pm$ 0.2	206.8	75.2 $\pm$ 0.2	0.17
$r = 150$	8192	83.7 $\pm$ 0.2	217.4	74.7 $\pm$ 0.1	0.13
	2048	82.8 $\pm$ 0.2	223.4	74.9 $\pm$ 0.1	0.17
	512	82.2 $\pm$ 0.3	217.7	75.0 $\pm$ 0.2	0.17
$r = 125$	8192	82.3 $\pm$ 0.4	229.0	74.2 $\pm$ 0.2	0.13
	2048	80.9 $\pm$ 0.3	238.6	74.1 $\pm$ 0.2	0.15
	512	80.9 $\pm$ 0.5	231.3	74.6 $\pm$ 0.3	0.16
$r = 100$	8192	80.3 $\pm$ 0.3	242.1	73.1 $\pm$ 0.4	0.14
	2048	78.9 $\pm$ 0.5	248.3	74.4 $\pm$ 0.1	0.18
	512	79.4 $\pm$ 0.3	241.2	74.2 $\pm$ 0.2	0.16
$r = 75$	8192	76.4 $\pm$ 0.6	265.6	72.9 $\pm$ 0.1	0.12
	2048	75.8 $\pm$ 0.3	269.3	73.8 $\pm$ 0.2	0.13
	512	76.5 $\pm$ 0.3	259.1	74.0 $\pm$ 0.1	0.13
$r = 50$	8192	69.9 $\pm$ 0.5	288.8	71.1 $\pm$ 0.1	0.12
	2048	70.2 $\pm$ 0.7	290.7	71.6 $\pm$ 0.2	0.13
	512	71.6 $\pm$ 0.6	280.3	72.2 $\pm$ 0.2	0.11
$r = 25$	8192	61.2 $\pm$ 0.4	309.1	69.1 $\pm$ 0.4	0.07
	2048	61.1 $\pm$ 0.4	307.9	68.4 $\pm$ 0.1	0.04
	512	64.6 $\pm$ 0.3	300.5	70.1 $\pm$ 0.1	0.10
$\bar{\text{LEOPARD}}$ (cascaded)					
$r = 275$	8192	85.5 $\pm$ 0.2	185.3	74.8 $\pm$ 0.1	0.20
	2048	85.5 $\pm$ 0.2	189.6	75.1 $\pm$ 0.1	0.17
	512	85.2 $\pm$ 0.2	193.4	75.4 $\pm$ 0.2	0.16
$r = 250$	8192	85.0 $\pm$ 0.3	198.7	74.9 $\pm$ 0.3	0.19
	2048	84.5 $\pm$ 0.3	204.1	74.8 $\pm$ 0.2	0.16
	512	84.6 $\pm$ 0.3	205.5	75.1 $\pm$ 0.1	0.14
$r = 225$	8192	84.2 $\pm$ 0.3	206.0	74.5 $\pm$ 0.1	0.20
	2048	83.8 $\pm$ 0.3	213.7	74.8 $\pm$ 0.1	0.15
	512	83.8 $\pm$ 0.3	214.0	75.3 $\pm$ 0.1	0.13
$r = 200$	8192	83.4 $\pm$ 0.2	215.1	74.6 $\pm$ 0.2	0.20
	2048	83.1 $\pm$ 0.2	223.9	74.8 $\pm$ 0.1	0.15
	512	82.9 $\pm$ 0.2	222.6	75.0 $\pm$ 0.2	0.12
$r = 175$	8192	82.3 $\pm$ 0.5	225.2	74.0 $\pm$ 0.2	0.19
	2048	81.3 $\pm$ 0.2	236.0	74.6 $\pm$ 0.3	0.13
	512	81.8 $\pm$ 0.2	232.1	74.8 $\pm$ 0.1	0.13
$r = 150$	8192	80.4 $\pm$ 0.5	239.4	74.0 $\pm$ 0.2	0.17
	2048	80.4 $\pm$ 0.4	245.0	74.7 $\pm$ 0.2	0.13
	512	80.1 $\pm$ 0.3	240.6	74.4 $\pm$ 0.2	0.14
$r = 125$	8192	79.1 $\pm$ 0.3	250.0	73.8 $\pm$ 0.2	0.16
	2048	78.5 $\pm$ 0.2	257.0	74.1 $\pm$ 0.2	0.14
	512	78.1 $\pm$ 0.4	253.0	74.4 $\pm$ 0.1	0.11
$r = 100$	8192	77.2 $\pm$ 0.4	263.3	73.9 $\pm$ 0.2	0.15
	2048	77.4 $\pm$ 0.3	264.1	74.4 $\pm$ 0.2	0.14
	512	76.5 $\pm$ 0.4	262.9	74.3 $\pm$ 0.2	0.11
$r = 75$	8192	73.8 $\pm$ 0.3	276.6	73.3 $\pm$ 0.1	0.12
	2048	73.3 $\pm$ 0.4	281.53	73.5 $\pm$ 0.2	0.12
	512	73.1 $\pm$ 0.3	274.7	74.0 $\pm$ 0.3	0.11
$r = 50$	8192	68.6 $\pm$ 0.5	293.2	71.9 $\pm$ 0.3	0.09
	2048	67.6 $\pm$ 0.3	297.6	71.8 $\pm$ 0.2	0.08
	512	68.6 $\pm$ 0.4	288.7	71.8 $\pm$ 0.2	0.08
$r = 25$	8192	60.3 $\pm$ 0.4	308.6	68.3 $\pm$ 0.2	0.04
	2048	62.4 $\pm$ 0.3	303.0	72.8 $\pm$ 0.2	0.11
	512	61.8 $\pm$ 0.5	304.5	69.0 $\pm$ 0.1	0.07

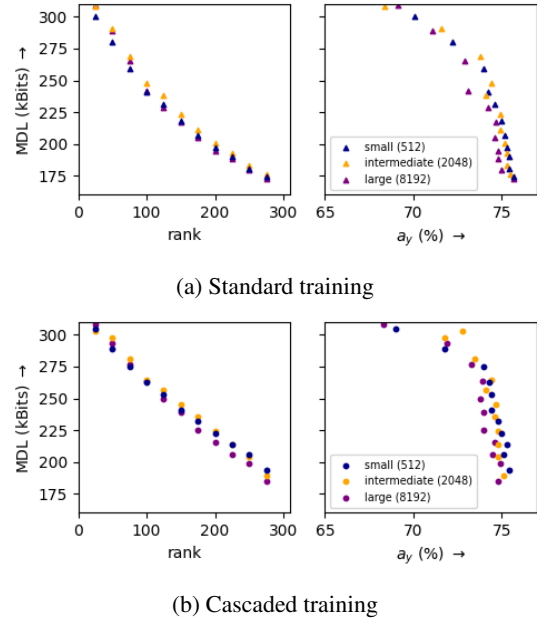


**Figure 10:** Race erasure in DIAL with  $\bar{\text{LEOPARD}}$  vs. rank of the feature space post-erasure (left) and Erasure–Utility trade-off (right) for different batch sizes used during training. The vertical axis, erasure strength as evaluated by MDL, is shared between the right and left panels.

## F Mixture of kernels

The analysis of results for various values of  $M$ , the number of kernels in the mixture of Eq. 8, shows that the improvement in performance becomes minimal beyond  $M = 2$ .

### F.1 GLOVE

**Table 9:** Gender erasure in GLOVE with Cascaded  $\bar{\text{LEOPARD}}$  for different number of kernels  $M$  in the mixture.

rank $r$	$M$	$a_z^{\text{bin}} \downarrow$ (%)	MDL $\uparrow$ (kBits)	$a_z^{\text{ter}} \downarrow$ (%)	$A_{50\%} \uparrow$	WS-353 $\uparrow$
200	1	66.1 $\pm$ 0.3	19.2	47.5 $\pm$ 0.9	0.82	0.61
	2	65.0 $\pm$ 0.7	19.6	45.3 $\pm$ 0.8	0.81	0.63
	5	65.2 $\pm$ 0.7	19.8	45.4 $\pm$ 0.7	0.81	0.64
150	1	57.3 $\pm$ 0.7	26.0	40.1 $\pm$ 0.6	0.80	0.60
	2	55.6 $\pm$ 0.2	27.0	38.7 $\pm$ 0.5	0.77	0.66
	5	55.9 $\pm$ 1.1	27.1	38.1 $\pm$ 0.6	0.78	0.64
100	1	53.5 $\pm$ 0.7	31.9	36.1 $\pm$ 1.4	0.77	0.57
	2	51.2 $\pm$ 0.4	32.5	35.0 $\pm$ 0.7	0.74	0.65
	5	51.0 $\pm$ 0.4	32.4	35.4 $\pm$ 0.7	0.74	0.64
50	1	51.3 $\pm$ 0.7	33.3	34.8 $\pm$ 0.7	0.72	0.54
	2	50.5 $\pm$ 0.4	34.8	34.5 $\pm$ 0.8	0.70	0.61
	5	50.4 $\pm$ 0.6	34.0	34.3 $\pm$ 1.0	0.70	0.60

### F.2 BIAS IN BIOS

**Table 10:** Gender erasure in BIAS IN BIOS with Cascaded  $\bar{\text{LEOPARD}}$  for different number of kernels  $M$  in the mixture.

rank $r$	$M$	$a_z \downarrow$ (%)	MDL	$a_y \uparrow$ (%)
200	1	64.1 $\pm$ 2.3	189.0	70.2 $\pm$ 0.3
	2	57.8 $\pm$ 1.1	191.0	68.2 $\pm$ 0.6
	5	57.3 $\pm$ 0.9	191.2	68.1 $\pm$ 0.6
	10	56.8 $\pm$ 0.5	190.2	68.5 $\pm$ 0.3
150	1	61.8 $\pm$ 1.2	190.1	67.9 $\pm$ 0.3
	2	57.2 $\pm$ 0.6	191.7	65.3 $\pm$ 0.6
	5	55.9 $\pm$ 0.3	192.2	65.5 $\pm$ 0.5
	10	55.6 $\pm$ 0.4	191.9	65.9 $\pm$ 0.3
100	1	61.0 $\pm$ 1.0	190.9	64.7 $\pm$ 0.5
	2	56.6 $\pm$ 0.8	192.6	61.2 $\pm$ 0.3
	5	55.1 $\pm$ 0.3	193.1	61.5 $\pm$ 0.6
	10	54.6 $\pm$ 0.2	192.7	61.9 $\pm$ 0.5
50	1	58.1 $\pm$ 1.9	192.1	57.8 $\pm$ 0.3
	2	54.5 $\pm$ 0.2	193.5	53.7 $\pm$ 0.5
	5	54.1 $\pm$ 0.2	193.5	54.1 $\pm$ 0.6
	10	54.0 $\pm$ 0.1	193.5	54.2 $\pm$ 0.5

### F.3 DIAL

**Table 11:** Race erasure in DIAL with Cascaded  $\bar{\text{LEOPARD}}$  for different number of kernels  $M$  in the mixture.

rank $r$	$M$	$a_z \downarrow$	MDL $\uparrow$	$a_y \uparrow$	DP $\downarrow$
75	1	74.3 $\pm$ 0.5	276.4	73.7 $\pm$ 0.1	0.10
	2	74.1 $\pm$ 0.4	275.1	74.3 $\pm$ 0.1	0.13
	5	73.3 $\pm$ 0.4	281.5	73.5 $\pm$ 0.2	0.12
	10	72.9 $\pm$ 0.7	281.3	73.9 $\pm$ 0.1	0.14
50	1	69.2 $\pm$ 0.3	294.1	72.7 $\pm$ 0.2	0.08
	2	67.7 $\pm$ 0.5	298.2	71.8 $\pm$ 0.2	0.07
	5	67.6 $\pm$ 0.3	297.6	71.8 $\pm$ 0.2	0.08
	10	67.0 $\pm$ 0.5	297.5	72.3 $\pm$ 0.3	0.08
25	1	63.0 $\pm$ 0.3	301.5	72.8 $\pm$ 0.1	0.10
	2	63.4 $\pm$ 0.5	300.0	73.1 $\pm$ 0.2	0.11
	5	62.4 $\pm$ 0.3	303.0	72.8 $\pm$ 0.2	0.11
	10	60.6 $\pm$ 0.5	307.0	71.6 $\pm$ 0.1	0.12
15	1	56.6 $\pm$ 0.3	309.9	68.6 $\pm$ 0.1	0.03
	2	56.9 $\pm$ 0.3	309.6	69.4 $\pm$ 0.1	0.04
	5	57.2 $\pm$ 0.3	309.0	70.2 $\pm$ 0.1	0.07
	10	54.2 $\pm$ 0.2	311.6	68.6 $\pm$ 0.1	0.07